Institut de Robòtica
i Informàtica Industrial

Consejo Superior de Investigaciones Científicas

Universitat Politècnica de Catalunya
BarcelonaTech

Juan Andrade Cetto
Director

Excelencia María de Maeztu
07/2017-06/2021

Agencia Estatal de Investigación

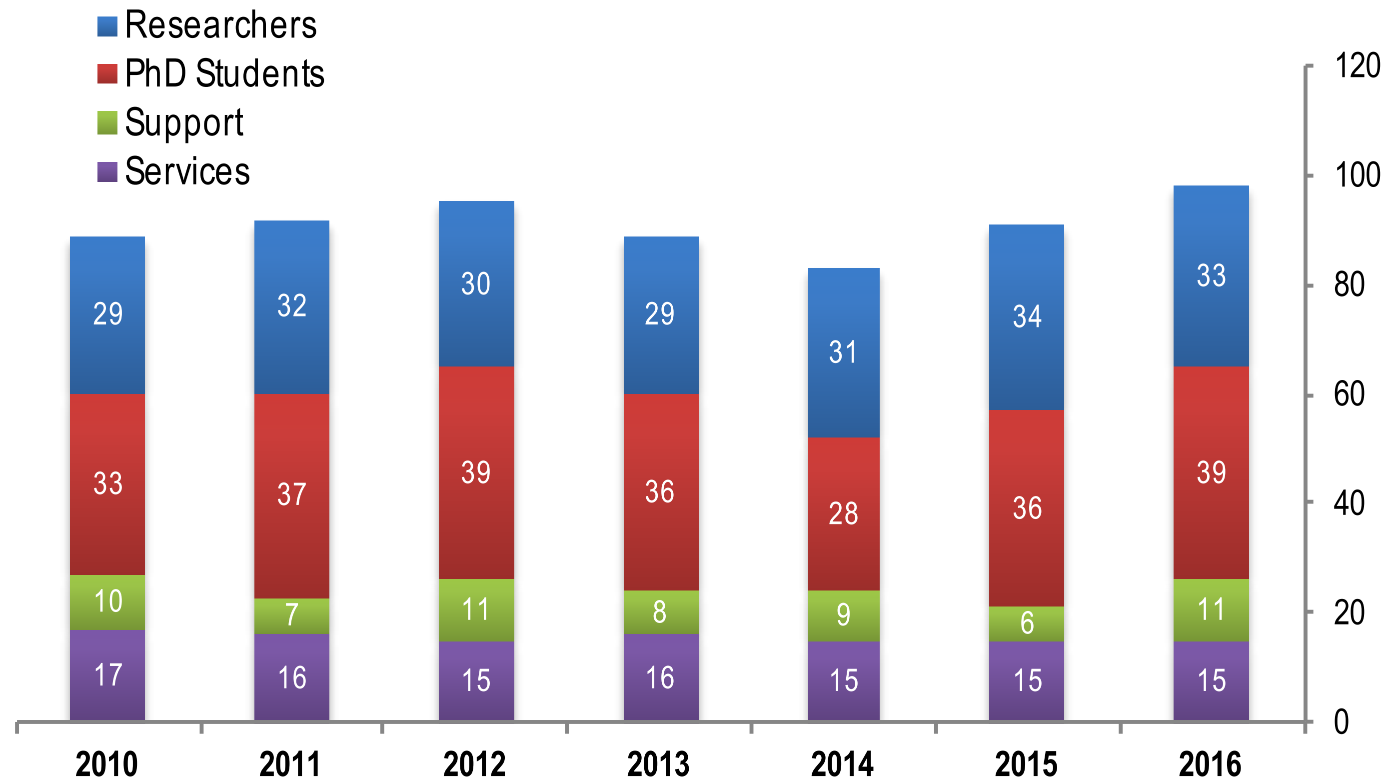

RESEARCH LINES

- Kinematics and Robot Design
- Mobile Robotics
- Perception and Manipulation
- Automatic Control

LABORATORIES

Peception and Manipulation Laboratory
Kinematics and Robot Design Laboratory
Mobile Robotics Laboratory
Barcelona Robot Laboratory
Fuel Cell Control Laboratory
Water-cycle Control Systems Laboratory

Kinematics and Robot Design

Researchers and faculty

Josep M Porta

Enric Celaya

Federico Thomas

Lluís Ros

Vicente Ruiz

Postdocs

Patrick Grosch

Mobile Robotics

Researchers and faculty

Alberto Sanfeliu

Juan Andrade

Rene Alquézar

Postdocs

Anaís Garrell

Joan Solá, RyC

Perception and Manipulation

Researchers and faculty

Carme Torras

Francesc Moreno

Guillem Alenyà

Maria Alberich

Pablo Jiménez

Postdocs

Antonio Agudo

Sergi Foix

Jan Funke

Aleksandar Jevtic

Lorenzo Porzi

Automatic Control

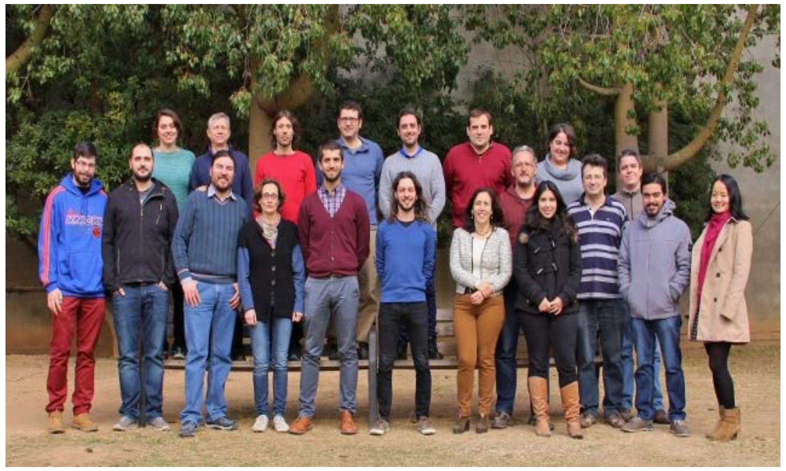

Researchers and faculty

Maria Serra

Gabriela Cembrano

Ramón Costa

Carlos Ocampo

Vicenç Puig

Sebastian Tornil

Postdocs

Joaquim Blesa, JdC

Attila Husar

Julio Luna

Congcong Sun

Human pose estimation
using CV and CNNs (CVPR, ICCV, IJCV)



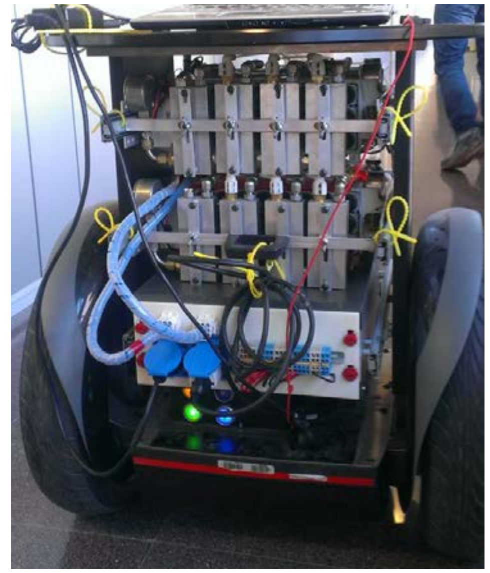
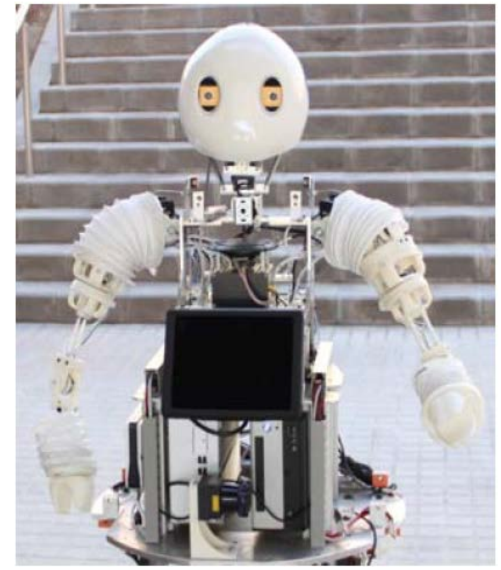


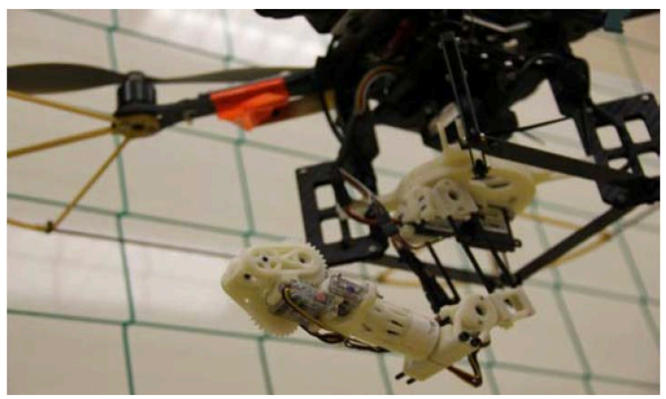
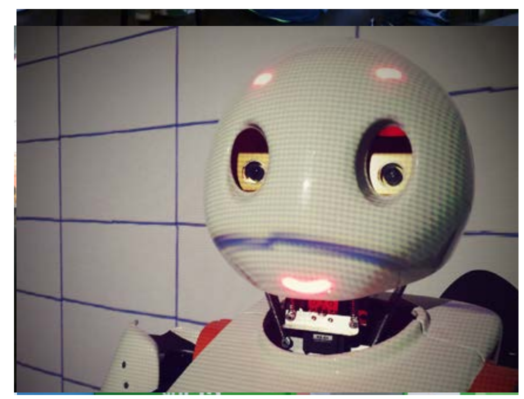

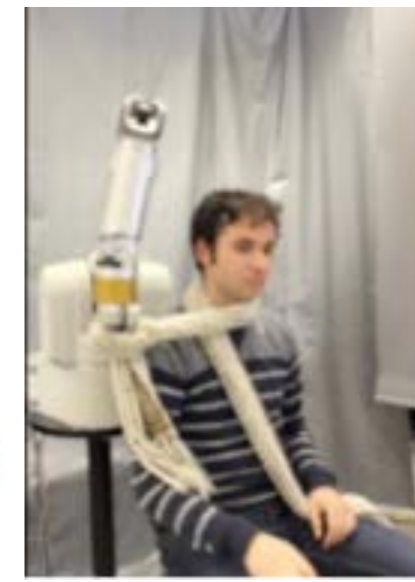

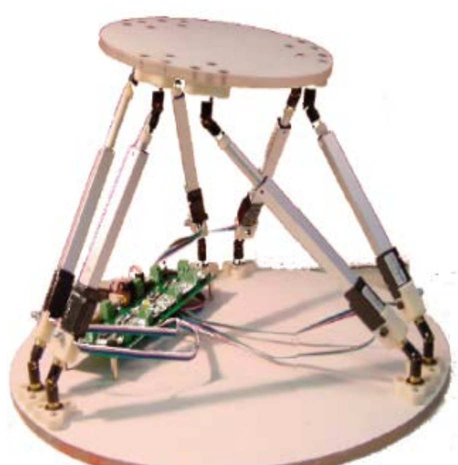

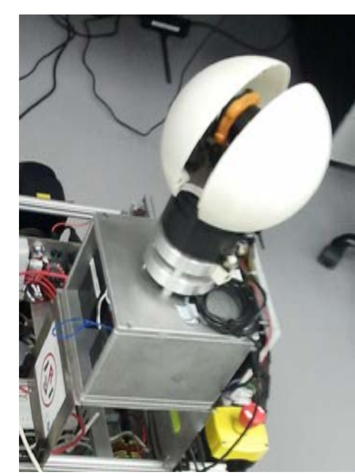


Current projects, Perception and Manipulation + Kinematics Groups

IMAGINE: Robots Understanding Their Actions by Imagining Their Effects
H2020-ICT-2016-1-731761

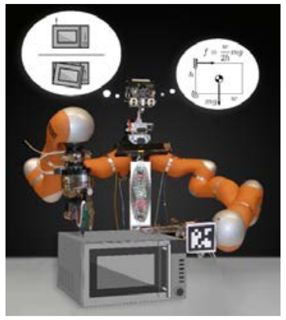

SOCRATES: SOcial Cognitive Robotics in The European Society
H2020-MSCA-ITN-721619

SOCRATES
Social Cognitive Robotics in The European Society

I-DRESS: Assistive interactive robotic system for support in dressing
PCIN-2015-147

RobInstruct: Instructing robots using natural communication skills
TIN2014-58178-R

RobCab: Control strategies for cable-driven robot for low-gravity simulation
DPI2014-57220-C2-2-P

Cloth manipulation learning from demonstrations

ERC Advanced Grant (ERC-2016-ADG-741930)

erc
European Research Council
Established by the European Commission

Current projects, Automatic Control Group

INN-BALANCE: INNovative Cost Improvements for BALANCE of Plant Components of Automotive PEMFC Systems
H2020-JTI-FCH-2016-1-735969

INCITE: Innovative controls for renewable sources integration into smart energy systems
H2020-MSCA-ITN-675318

EFFIDRAIN: Efficient Integrated Real-time Control in Urban Drainage and Wastewater Treatment Plants for Environmental Protection
LIFE14 ENV/ES/000860

GRACeFUL: Global systems Rapid Assessment tools through Constraint FUnctional Languages
H2020-FETPROACT-2014-640954

DEOCS: Monitorización, diagnostico y control tolerante a fallos de sistemas ciberfísicos con métodos basados en datos
DPI2016-76493-C3-3-R

MICAPEM: Parameter estimation, diagnosis and control for the improvement of efficiency and durability of PEM fuel cells
DPI2015- 69286-C3-2-R

Current projects, Mobile Robotics Group

AEROARMS: AErial RObotics System integrating multiple ARMS and advanced manipulation capabilities for inspection and maintenance
H2020-ICT-2014-1-644271

ECHORD++: European Clearing House for Open Robotics Development Plus Plus
FP7-ICT-2011-9-601116

Cargo-ANTS: Cargo handling by Automated Next generation Transportation Systems for ports and terminals
FP7-SST-2013-RTD-1-605598

LOGIMATIC: Tight integration of EGNSS and on-board sensors for port vehicle automation
H2020-Galileo-2015-1-687534

ColRobTransp: Colaboración robots-humanos para el transporte de productos en zonas urbanas
DPI2016-78957-R

Visual Guidance of Unmanned Aerial Manipulators

Juan Andrade Cetto

Based on the work of:
Angel Santamaria Navarro

with contributions from:
L. Bascetta, V. Cacace, Y.R. Esteves, P. Grosch, V. Kumar, V. Lippiello,
A. Loianno, D. Lunni, P. Rocco, R. Rossi, and J. Solà, and M.A. Trujillo, A. Viguria

Institut de Robòtica i Informàtica Industrial
CSIC
UPC

ARCAS
AEROARMS

Aerial Robots

Unmanned Aerial Manipulators (**UAM**)

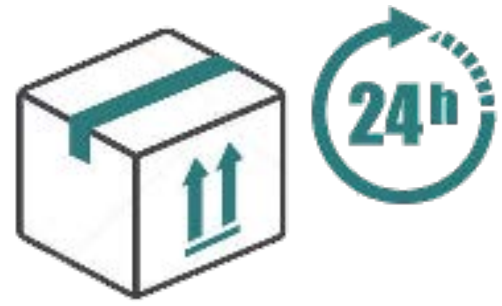

Goal: Autonomous operation

Challenges

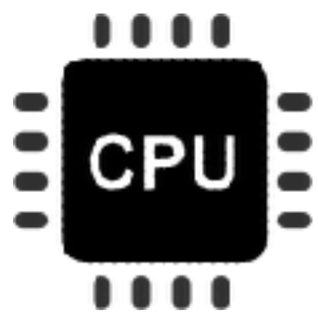

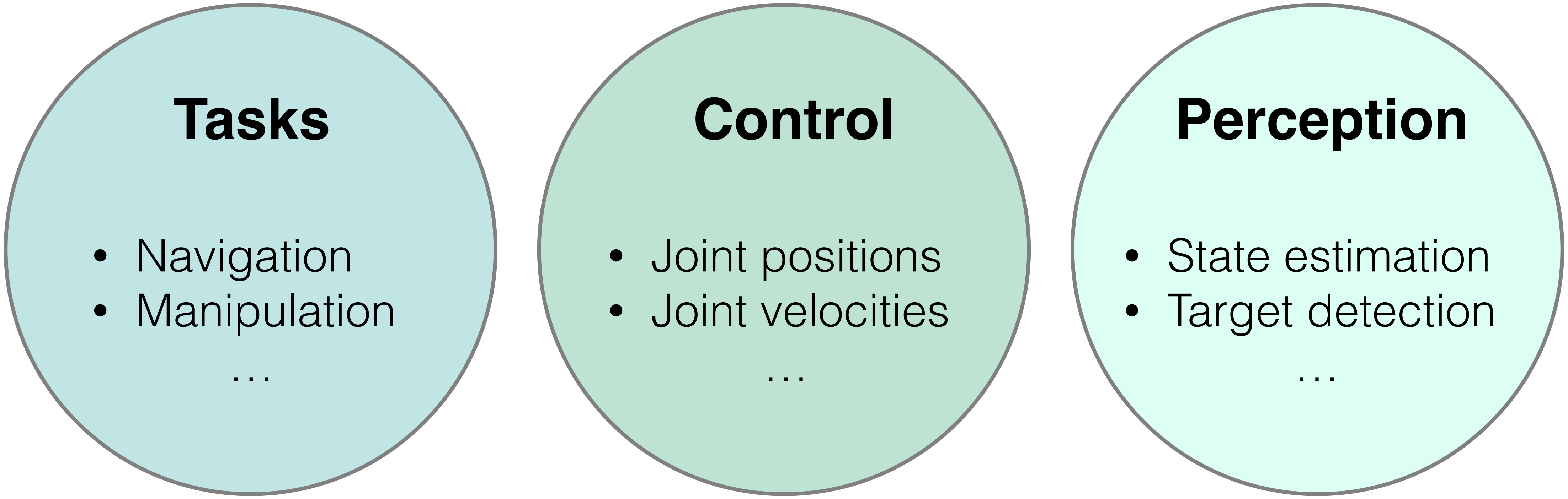
Tasks
• Navigation
• Manipulation
…
Control
• Joint positions
• Joint velocities
…
Perception
• State estimation
• Target detection
…

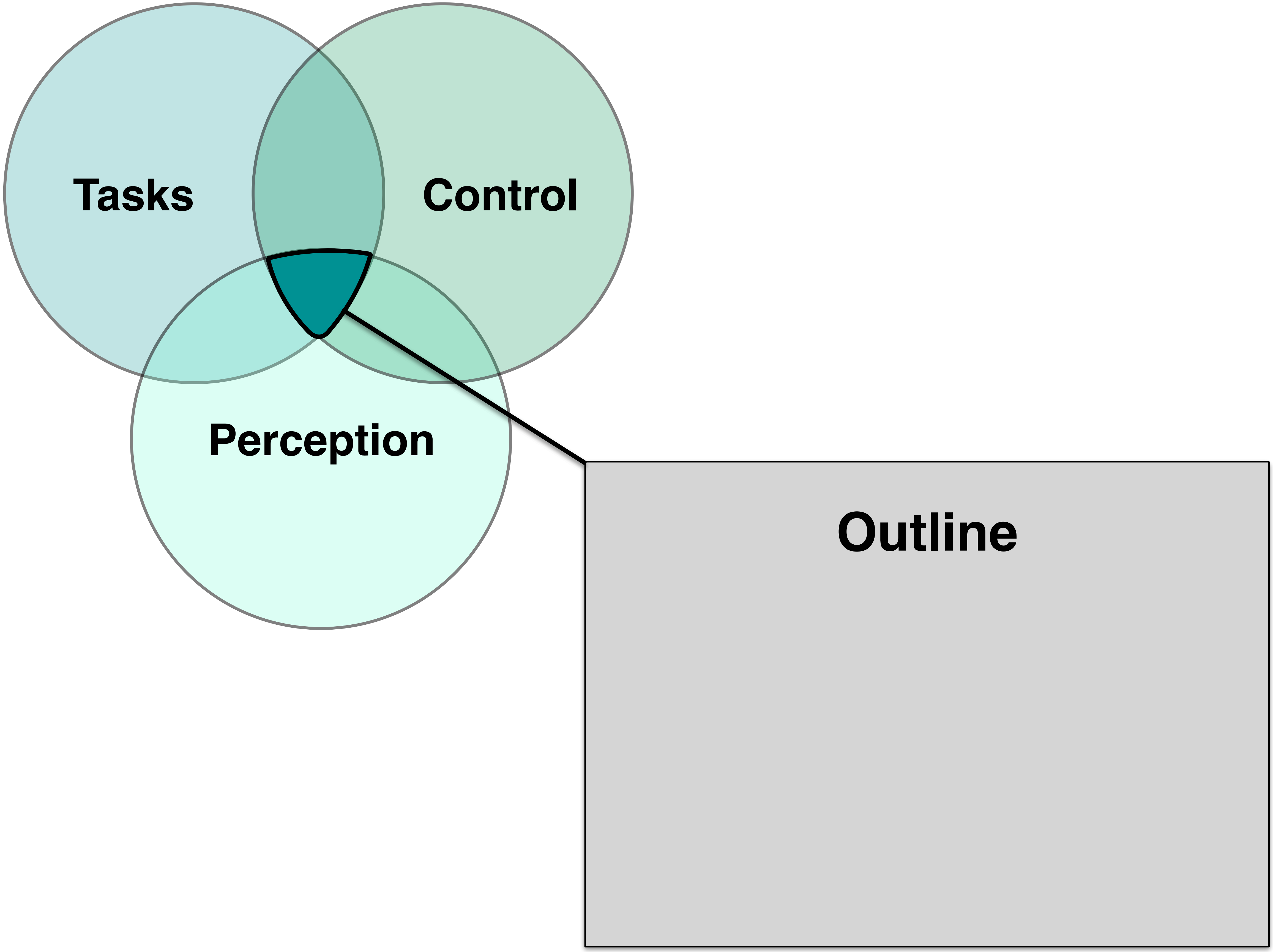
Tasks
Control
Perception
Outline

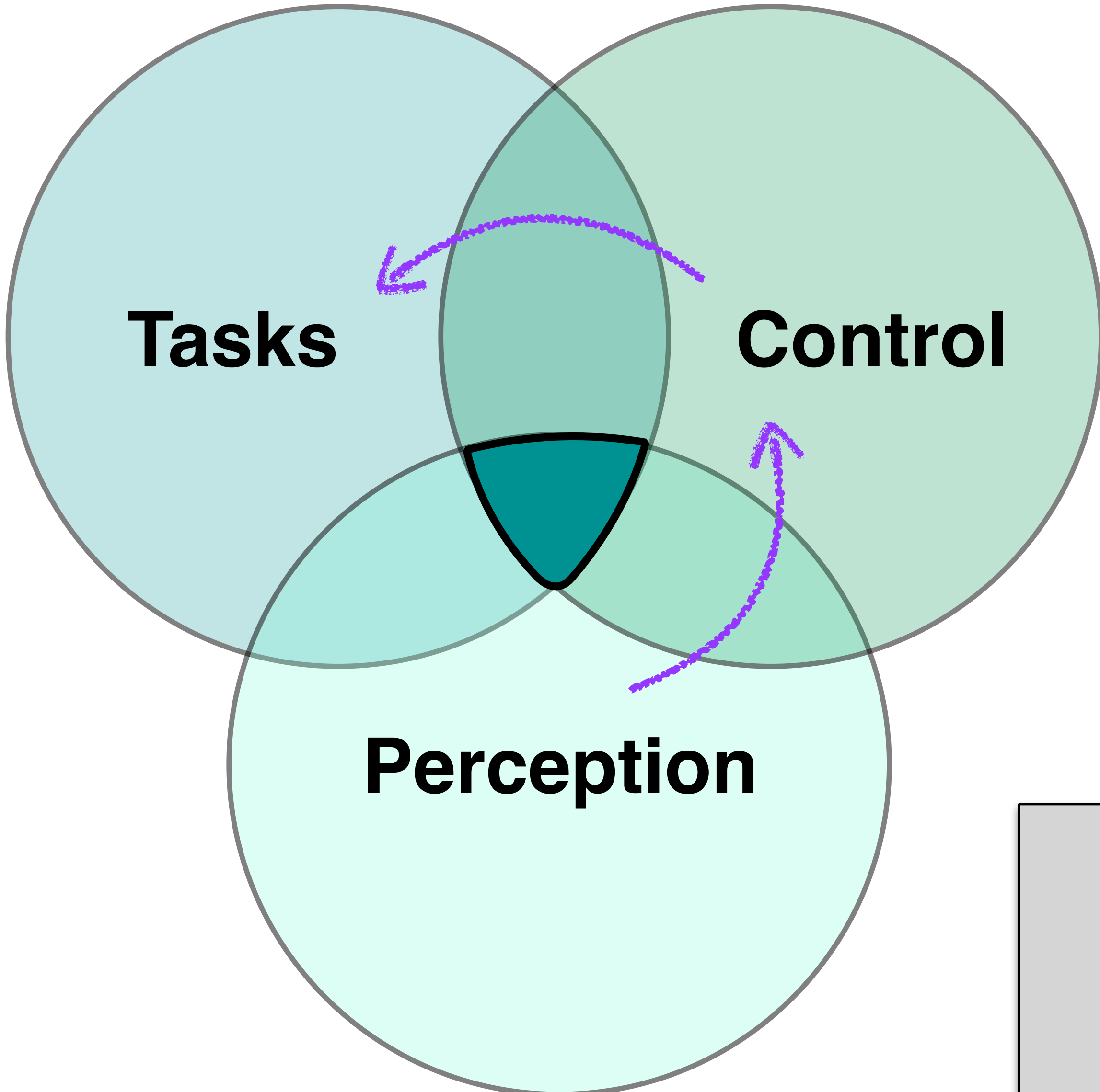

Outline

- Robot state estimation
- Visual servo control
- Task control
- Conclusions

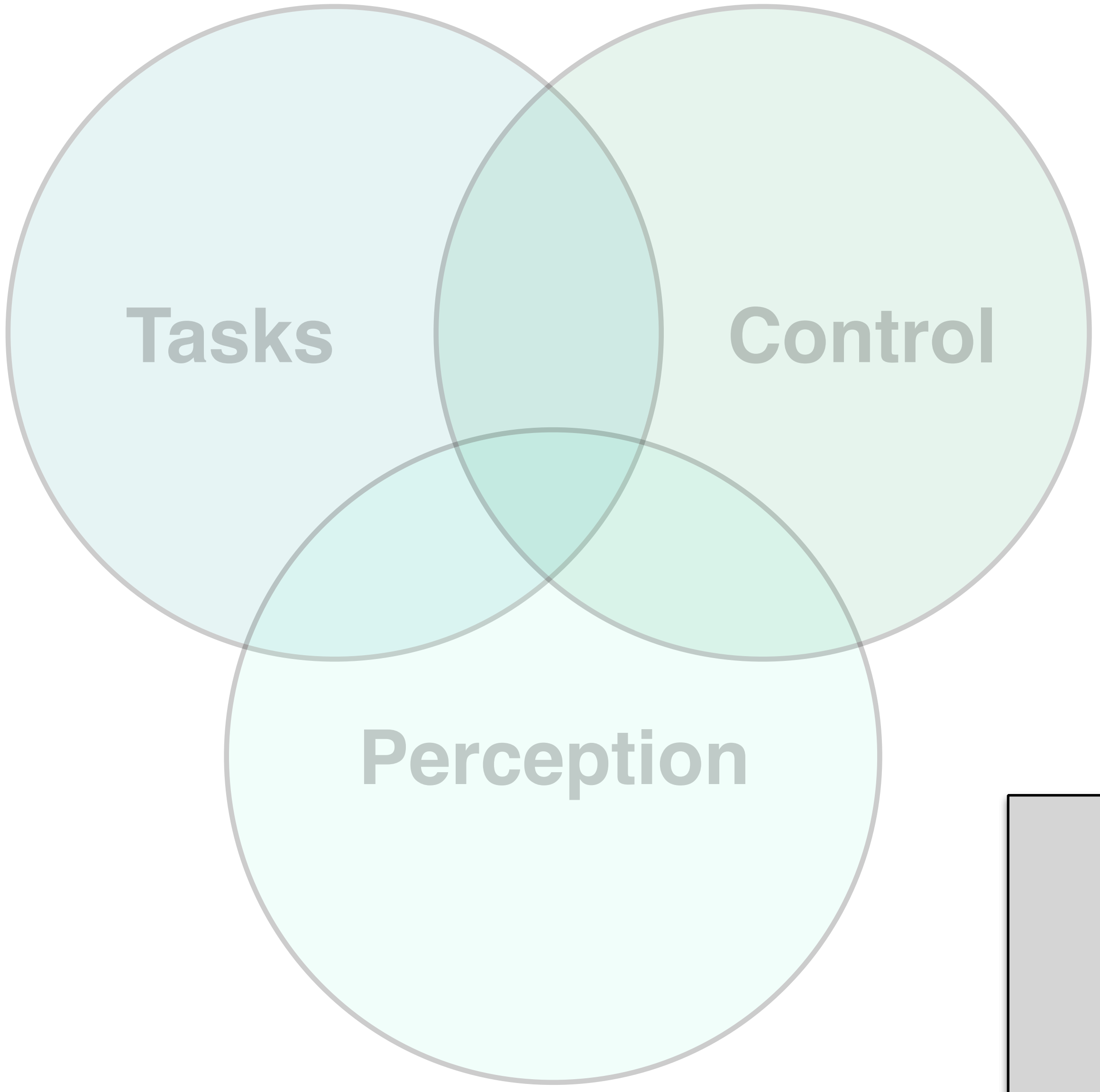

Outline

- Robot state estimation
- Visual servo control
- Task control
- Conclusions

Robot state
- position
- velocity
- acceleration

State estimation methods

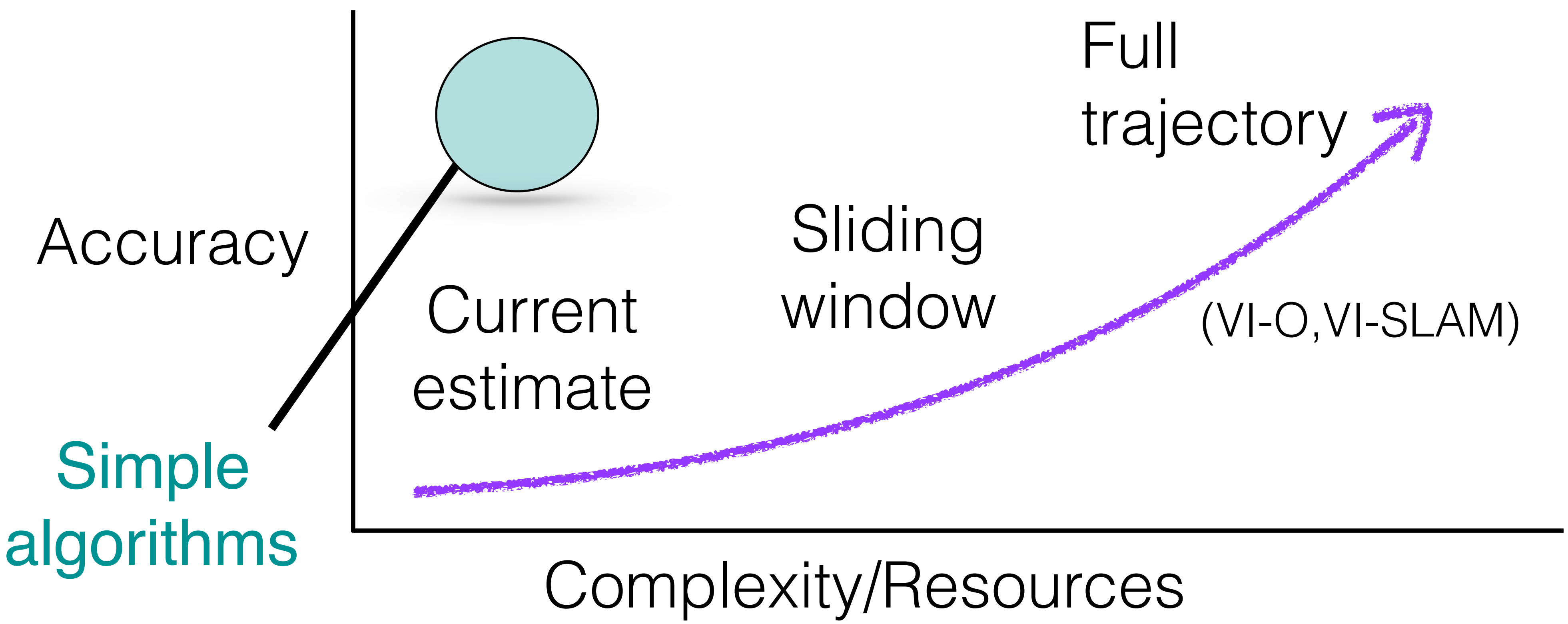

Target: UAM platforms

- Light-weight and low-cost sensors
- Limited CPU

System setup

Visual-inertial

- Light weight, low cost
- Account for system dynamics
- Register gravity vector

IMU

- Accelerometers
- Gyroscopes

Smart camera (SC)

- 2D raw optical flow
- Height (sonar)
- 2D linear velocities

IR Ranger

- Height

Setting A

- IMU
- SC: 2D linear vel.
- SC: Sonar range

Setting B

- IMU
- SC: 2D opt. flow
- IR range

Design

Simplicity vs. Performance: What's the trade-off?

Benchmark Kalman filter variants

(B1)
Extended (**EKF**)
vs.
Error-State (**ESKF**)

(B2)
ESKF: Orientation error definition
(global, local)

(B3) (B4)
Integration approx.
(taylor, quaternion)

Filters (B1)

- Extended Kalman Filter (EKF): Direct estimation of $\boldsymbol{x}_t$

$$\longrightarrow \boldsymbol{x}_t = \begin{bmatrix} \boldsymbol{p}_t & \boldsymbol{v}_t & \boldsymbol{q}_t & \boldsymbol{a}_{bt} & \boldsymbol{\omega}_{bt} \end{bmatrix}^\top$$

- Error State Kalman Filter (ESKF):

$$\boldsymbol{x}_t = \boldsymbol{x} \oplus \delta\boldsymbol{x} \qquad \boldsymbol{x} = \begin{bmatrix} \boldsymbol{p} & \boldsymbol{v} & \boldsymbol{q} & \boldsymbol{a}_b & \boldsymbol{\omega}_b \end{bmatrix}^\top$$

$$\longrightarrow \delta\boldsymbol{x} = \begin{bmatrix} \delta\boldsymbol{p} & \delta\boldsymbol{v} & \delta\boldsymbol{\theta} & \delta\boldsymbol{a}_b & \delta\boldsymbol{\omega}_b \end{bmatrix}^\top$$

(B2) ESKF: Orientation error definition

$$\text{global error (GE)}: \boldsymbol{q}_t = \delta\boldsymbol{q} \otimes \boldsymbol{q}$$

$$\text{local error (LE)}: \boldsymbol{q}_t = \boldsymbol{q} \otimes \delta\boldsymbol{q}$$

Continuous system kinematics

$$\dot{\boldsymbol{x}} = f(\boldsymbol{x}, \boldsymbol{u}) \quad \text{(nonlinear)}$$

$$\int_{(k-1)\Delta t}^{k\Delta t} f(\boldsymbol{x}, \boldsymbol{u})$$

↓

Discrete system kinematics

$$\boldsymbol{x}_k \approx \boldsymbol{F}\boldsymbol{x}_{k-1} + \boldsymbol{B}\boldsymbol{u}\triangle t$$

(B3) Taylor series with different truncation grade

$$\boldsymbol{F} = e^{\boldsymbol{A}\triangle t} \longrightarrow \boldsymbol{F}_N \approx \boldsymbol{I} + \boldsymbol{A}\triangle t + \frac{1}{2}\boldsymbol{A}^2\triangle t^2 + \ldots + \frac{1}{N}\boldsymbol{A}^N\triangle t^N$$

(B4) Quaternion integration

Q0F: $\boldsymbol{q}_k \approx \boldsymbol{q}_{k-1} \otimes \boldsymbol{q}(\boldsymbol{\omega}_{k-1}\triangle t)$

Q0B: $\boldsymbol{q}_k \approx \boldsymbol{q}_{k-1} \otimes \boldsymbol{q}(\boldsymbol{\omega}_{k}\triangle t)$

Q1: $\boldsymbol{q}_k \approx \boldsymbol{q}_{k-1} \otimes \left(\boldsymbol{q}(\overline{\boldsymbol{\omega}}\triangle t) + \frac{\triangle t^2}{24}\begin{bmatrix} 0 \\ \boldsymbol{\omega}_{k-1} \times \boldsymbol{\omega}_k \end{bmatrix}\right)$

Simulations

Setting A

- IMU
- SC: 2D linear vel.
- SC: Sonar range

X, Y and Yaw non observable: Odometer

Acc. Biases observability depending on platform tilt

Ang. Vel. Bias (Yaw) observable after long period!

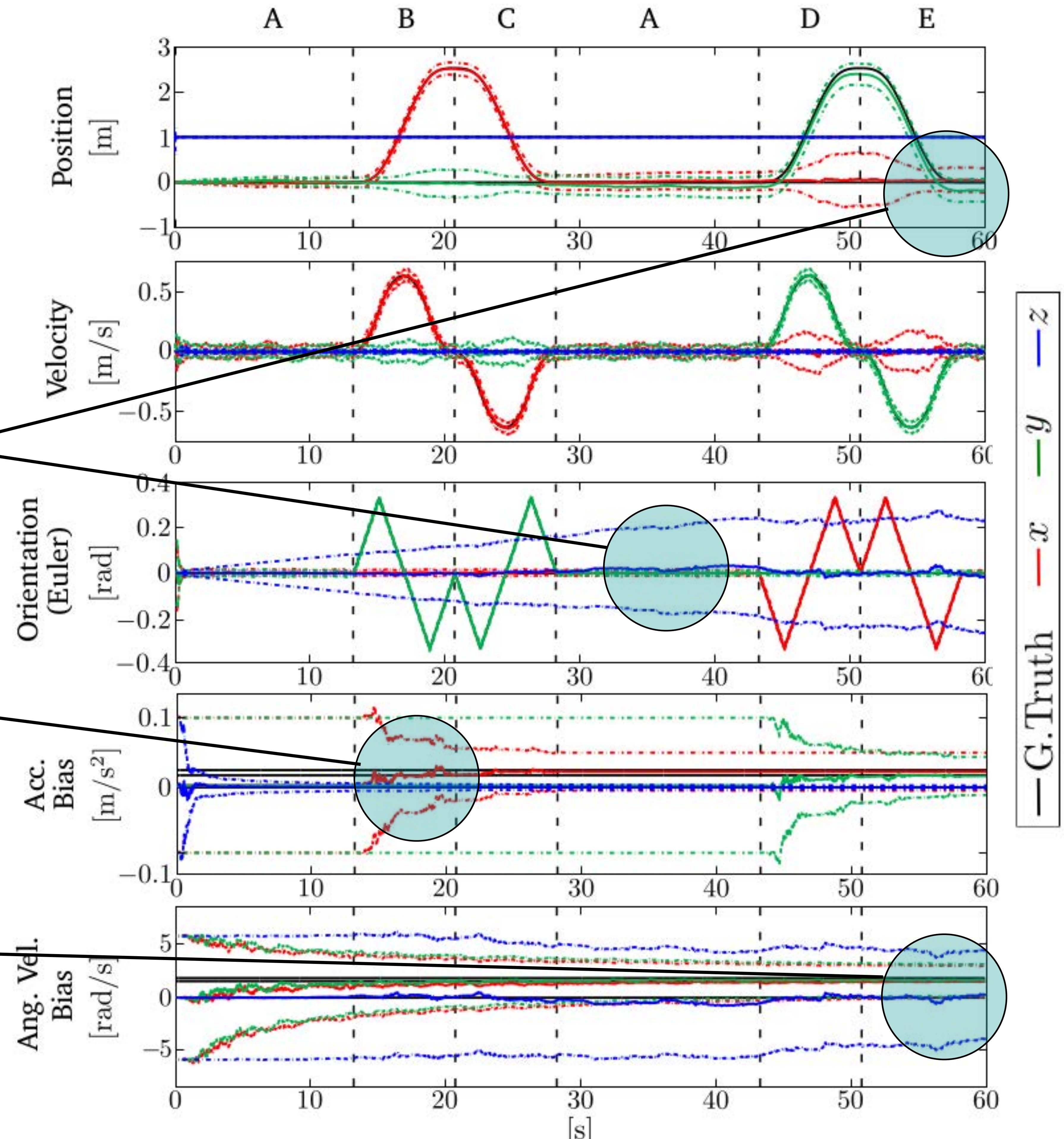

Simulations

Setting B

- IMU
- SC: 2D opt. flow
- IR range

Estimation error after 10min flights of 500m in straight line

Error Component ϵ_i	Filter Variant										
	EKF F_1 Q0F LE	EKF F_1 Q0B LE	EKF F_1 Q1 LE	EKF F_2 Q1 LE	EKF F_3 Q1 LE	ESKF F_1 Q0F GE	ESKF F_1 Q0B GE	ESKF F_1 Q1 GE	ESKF F_2 Q1 GE	ESKF F_3 Q1 GE	ESKF F_1 Q0F LE
x [m]	10.54	10.48	10.30	10.26	10.26	10.58	10.37	10.13	10.12	10.12	10.38
y [m]	11.13	11.07	10.85	10.81	10.81	11.00	10.82	10.55	10.58	10.58	10.91
z [mm]	7	6	7	6	6	7	7	7	7	7	7

Root Mean Squared Error (RMSE) over 20 experiments

Real robot experiments

Setting A

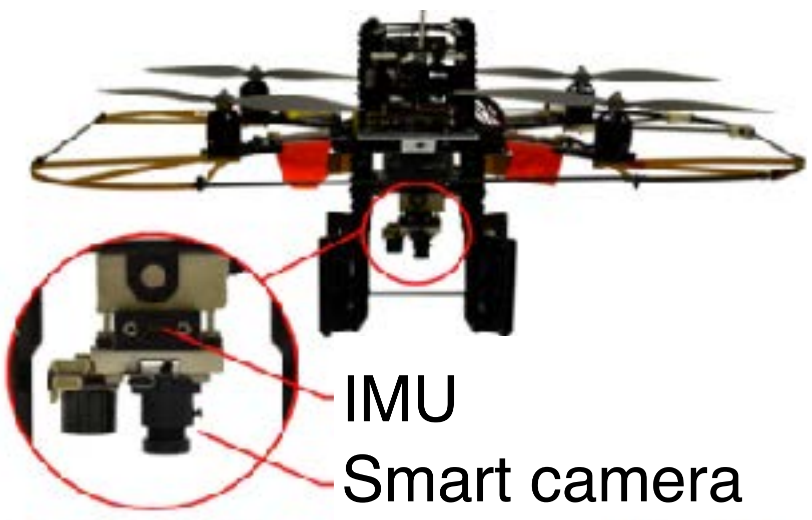

- Accelerometers
- Gyroscopes
- 2D linear velocities
- Ranger (sonar)

Setting B

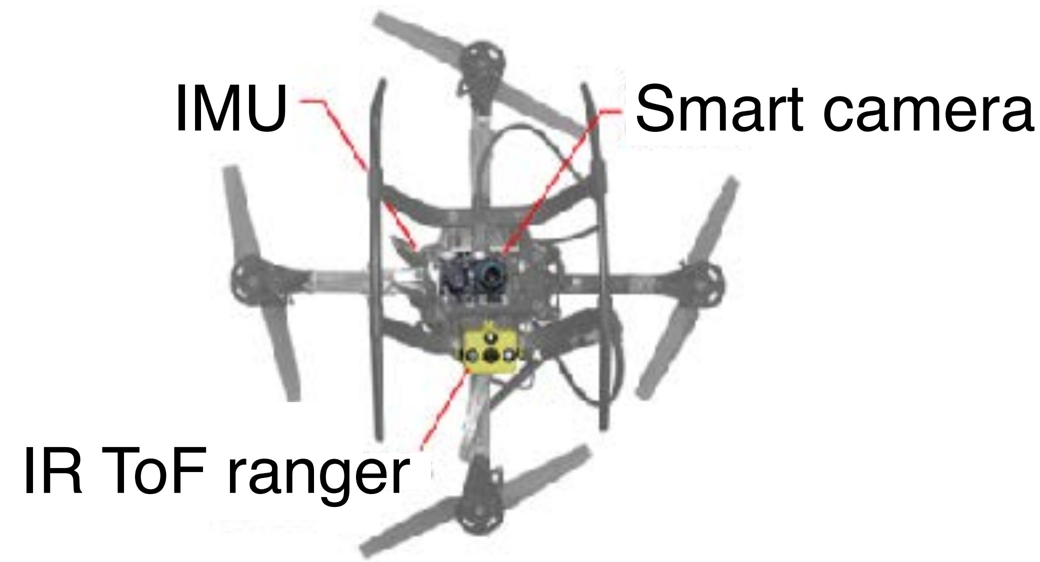

- Accelerometers
- Gyroscopes
- 2D raw optical flow
- Ranger (IR)

Control loop
with a nonlinear
tracking controller on $\mathcal{SE}(3)$

Setting A

Indoor

Outdoor

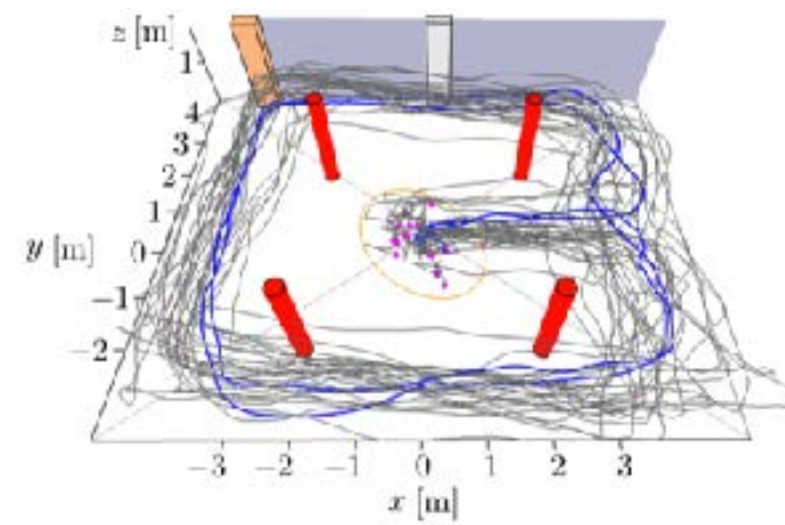

0.5m error after 2min flight (avg.)

Setting B Research stay at UPenn

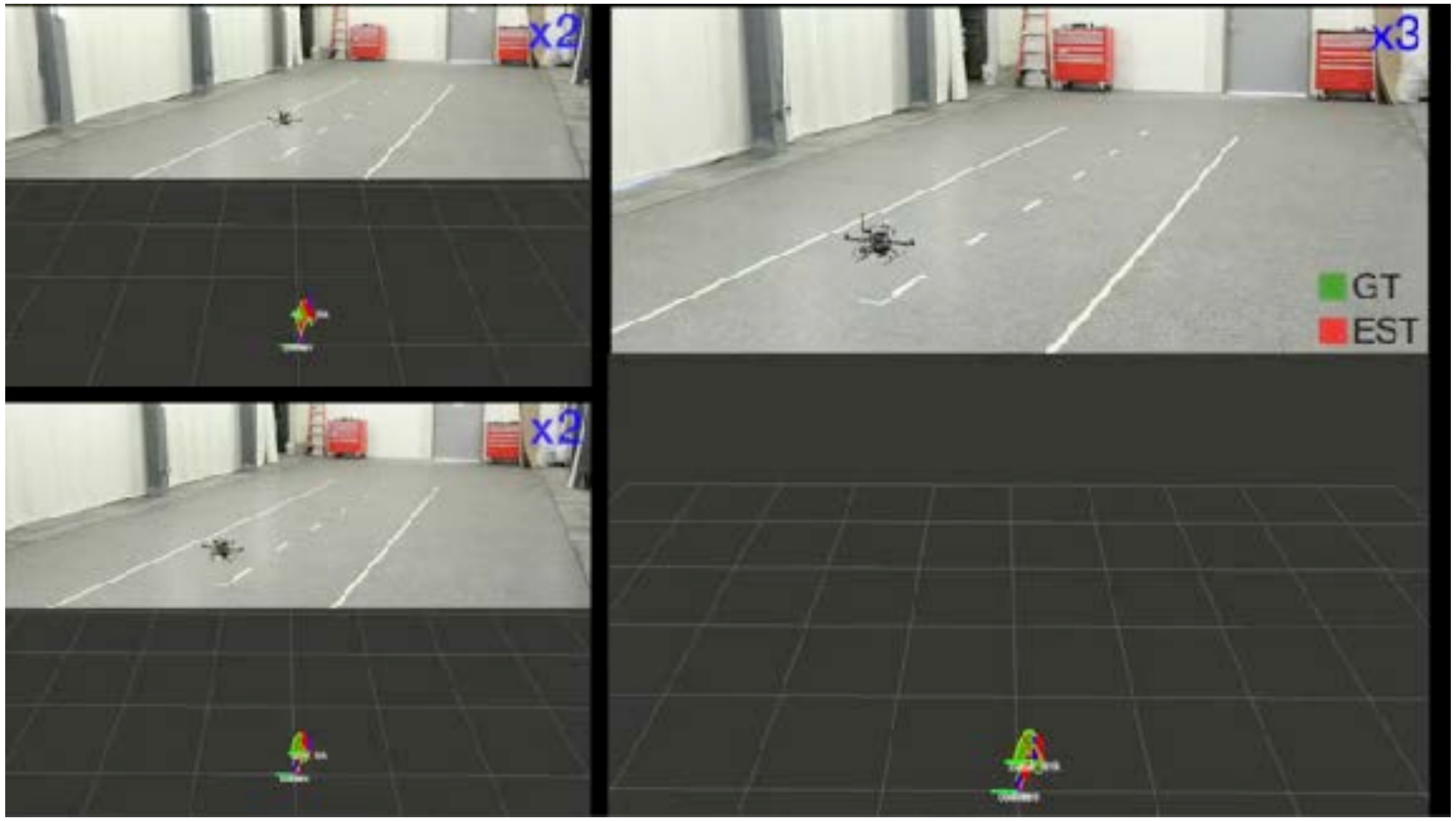

Error analysis

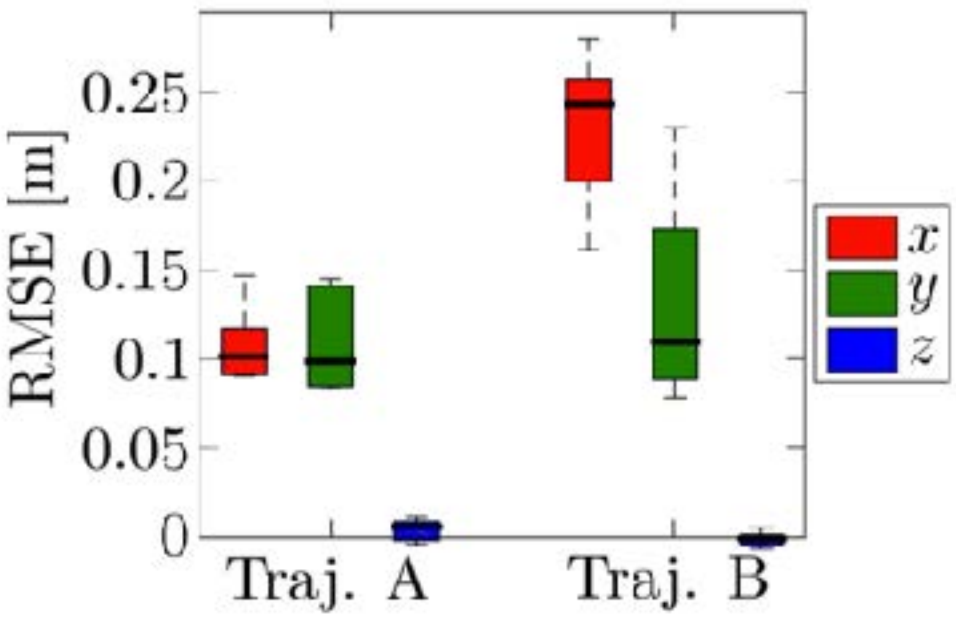

2 traj. with 25 runs each.

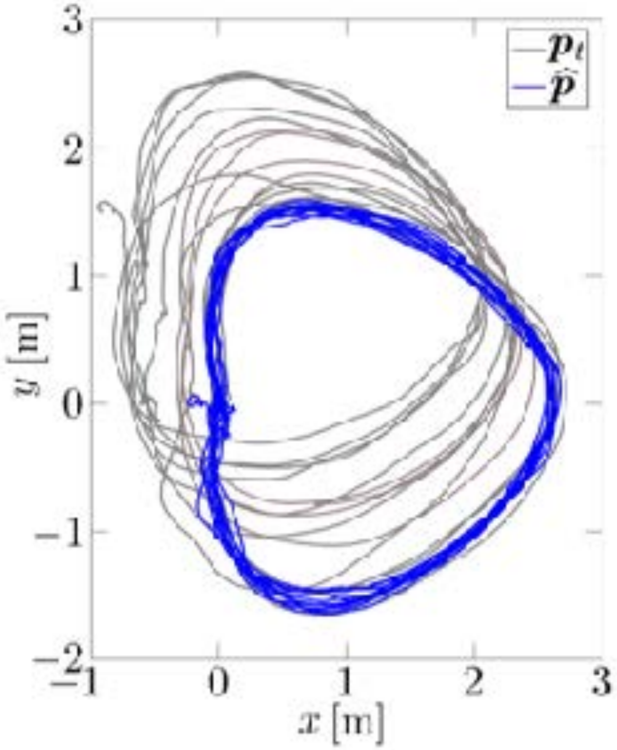

10 min flight (full battery discharge)

RMSE (m) [0.47 0.67 0.035]

State estimation remarks

- Light-weight, low-cost sensors and low-complexity algorithms
- Benchmark of Kalman filter variants:
  - All filters perform equally (@100Hz)
  - Acceptable errors for autonomous navigation

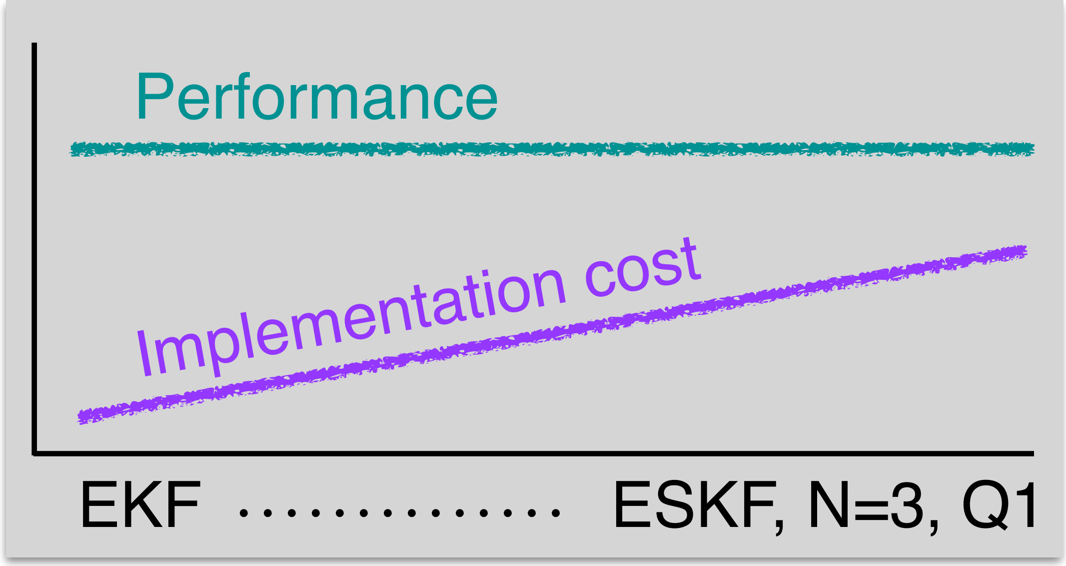

Santamaria-Navarro, A., Sola, J., and Andrade-Cetto, J., High-frequency MAV state estimation using low-cost inertial and optical flow measurement units, 2015 IEEE/RSJ International Conference on Intelligent Robots and Systems (IROS), pp. 1864-1871, Hamburg, Germany.

Santamaria-Navarro, A., Loianno, G., Solà, J., Kumar, V., and Andrade-Cetto, J., Autonomous navigation of micro aerial vehicles: State estimation using fast and low-cost sensors. Submitted to Autonomous Robots.

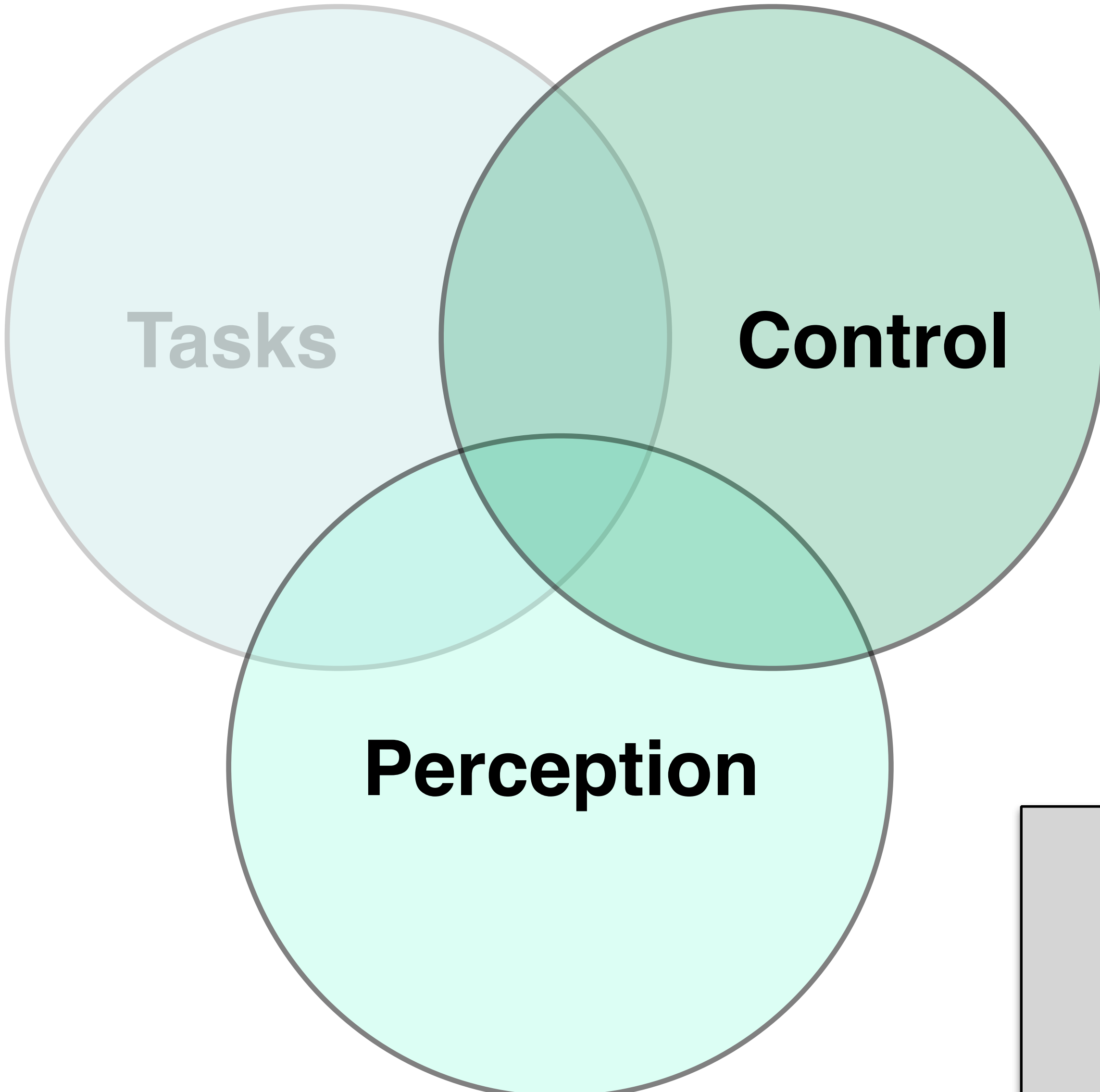

Outline

- Robot state estimation
- Visual servo control
- Task control
- Conclusions

Principle

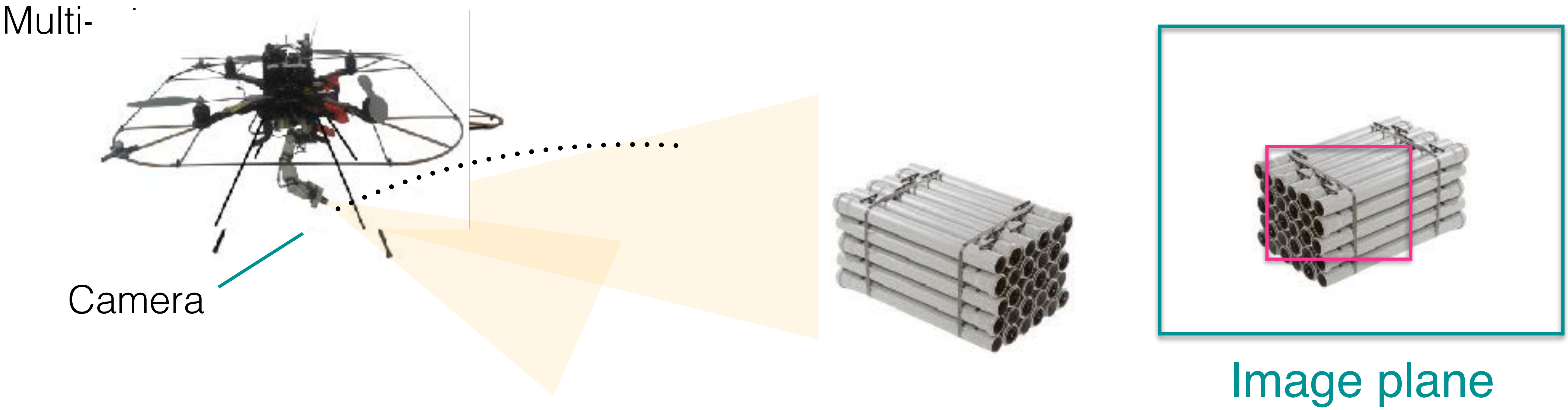

Objective: drive the robot using visual information

Reduce the **error** between current and desired points of view

$$\boldsymbol{e}(t) = \boldsymbol{s}(t) - \boldsymbol{s}^{d}$$

$$\boldsymbol{e} = -\lambda \dot{\boldsymbol{e}} = -\lambda \boldsymbol{J}\,{}^{c}\boldsymbol{\vartheta}$$

- Position-based (PBVS)
- Image-based VS (IBVS)
- Hybrid VS (HVS)

6DoF camera vel. ${}^{c}\boldsymbol{\vartheta} = -\lambda \boldsymbol{J}^{+}\boldsymbol{e}$

Schemes

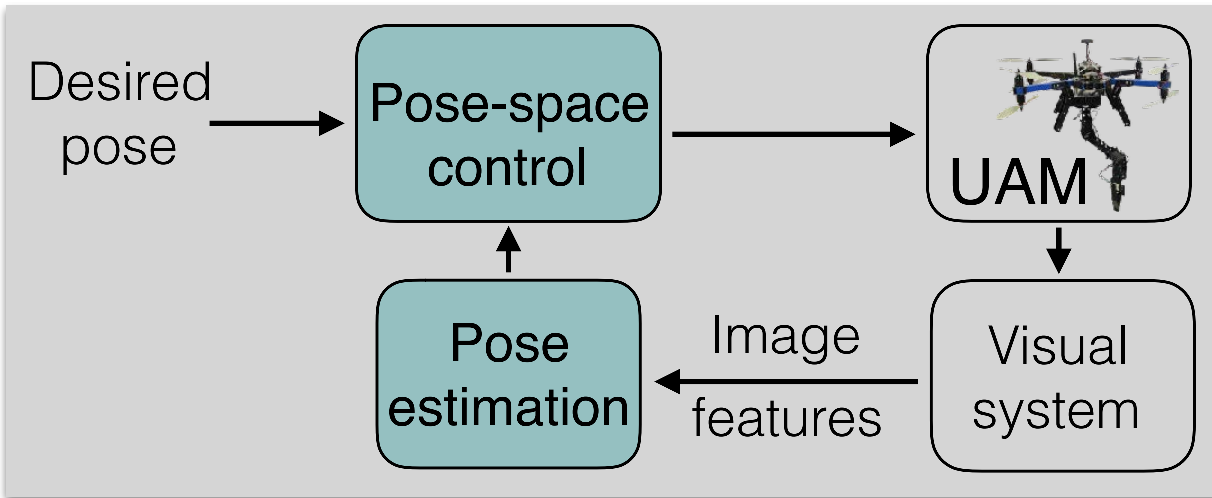

PBVS: Position-based visual servo

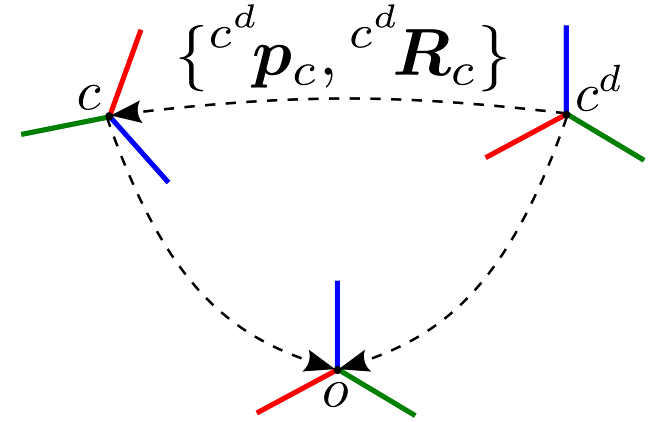

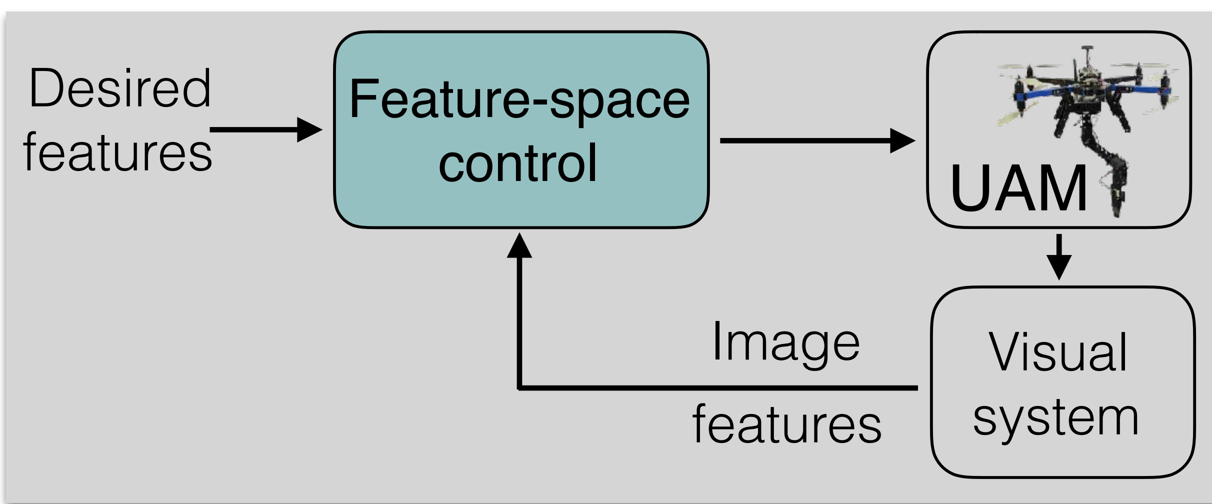

IBVS: Image-based visual servo

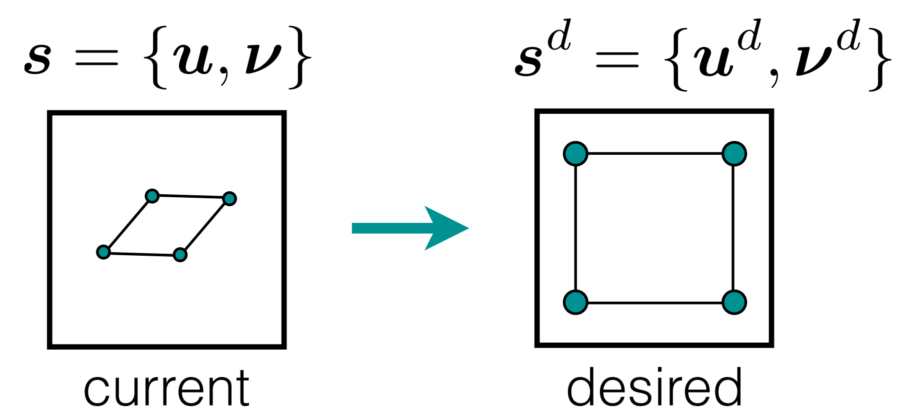

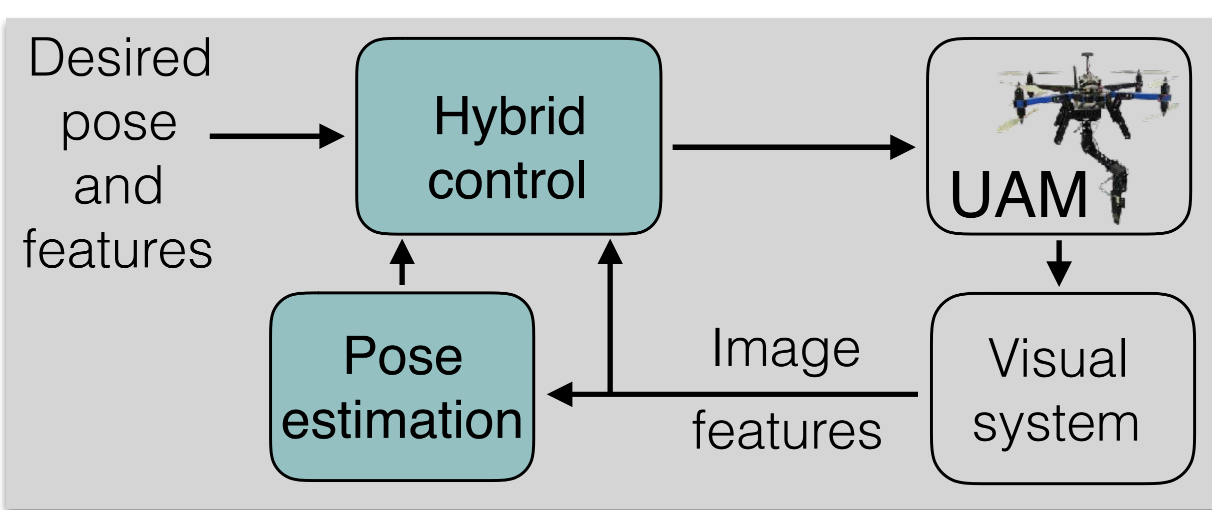

HVS: Hybrid visual servo

PBVS + IBVS

IBVS: Image-based visual servo

- Image Jacobian depends on focal length

$$ {}^{c}\boldsymbol{\vartheta} = -\lambda \boldsymbol{J}^{+} \boldsymbol{e} $$

$$ \boldsymbol{J} = [\boldsymbol{J}_1^\top \ldots \boldsymbol{J}_n^\top]^\top \quad (n \text{ features}) $$

$$ \boldsymbol{J}_j = \begin{bmatrix} -\frac{1}{z} & 0 & \frac{u}{z} & u\nu & -(1+u^2) & \nu \\ 0 & -\frac{1}{z} & \frac{\nu}{z} & (1+\nu^2) & -u\nu & -u \end{bmatrix} $$

UIBVS: Uncalibrated image-based visual servo

Uncalibrated image-based visual servo (UIBVS)

- Drawing inspiration on EPnP and UPnP algorithms

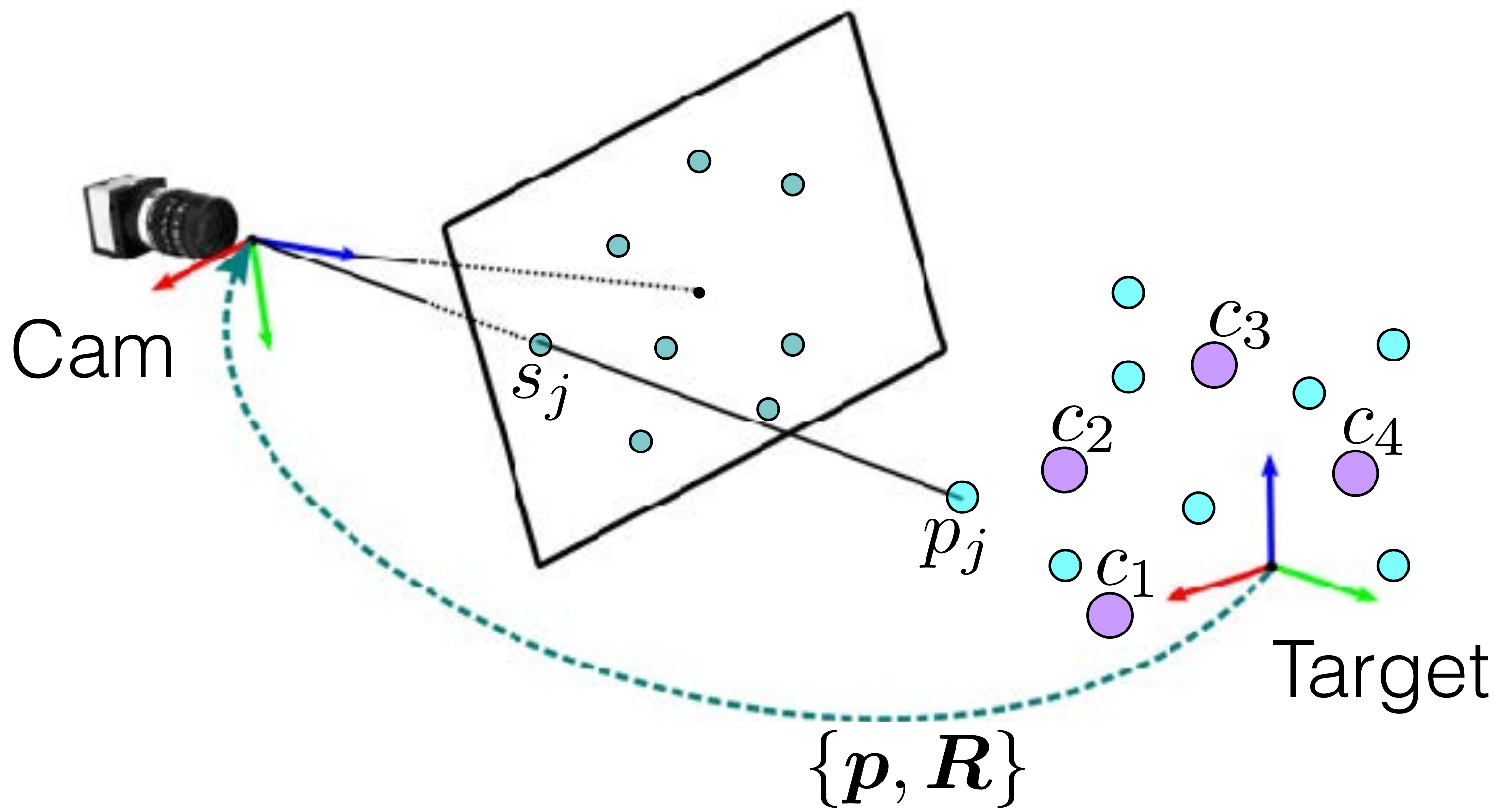

Set 4 control points (**CP**) as a basis of the target frame

Target pose **=** 3D coordinates of CP in camera frame

- Each target features as a function of CP
- Perspective projection equations

$$\boldsymbol{M}\boldsymbol{x} = \boldsymbol{0}$$ 2D-3D correspondences

12 unknowns $\boldsymbol{x} = [x_1,\ y_1,\ z_1/\alpha, \ldots, x_4,\ y_4,\ z_4/\alpha]^\top$

↓ SVD

$$\boldsymbol{x} = \beta\boldsymbol{\mu}$$

$\boldsymbol{\mu}$: Eigenvector of null eigenvalue of $\boldsymbol{M}^\top\boldsymbol{M}$

↓

Solve for α and β

Distances between CP must be preserved (+6 constraints)

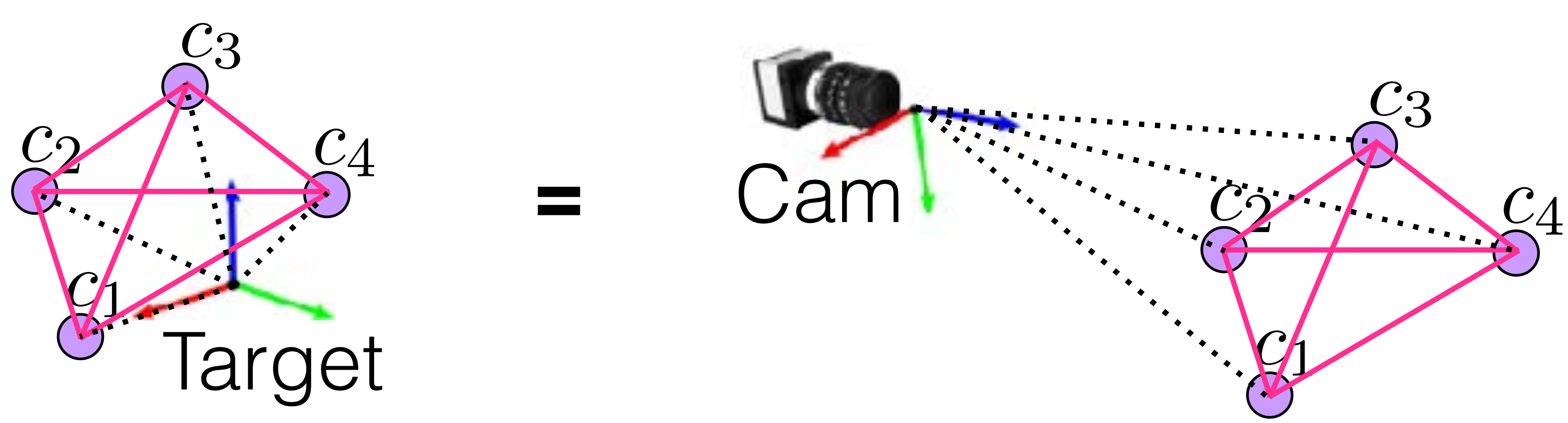

- Uncalibrated image Jacobian

$$\boldsymbol{J}_j = \begin{bmatrix} \frac{-1}{\beta\mu_z} & 0 & \frac{\mu_x}{\alpha\beta\mu_z^2} & \frac{\mu_x\mu_y}{\alpha\mu^2} & \frac{-\mu_x^2-\alpha^2\mu_z^2}{\alpha\mu_z^2} & \frac{\mu_y}{\mu_z} \\ 0 & \frac{-1}{\beta\mu_z} & \frac{\mu_y}{\alpha\beta\mu_z^2} & \frac{\mu_y^2+\alpha^2\mu_z^2}{\alpha\mu_z^2} & \frac{-\mu_x\mu_y}{\alpha\mu_z^2} & \frac{-\mu_x}{\mu_z} \end{bmatrix}$$

$$\boldsymbol{J} = [\boldsymbol{J}_1^\top \ldots \boldsymbol{J}_4^\top]^\top$$

6DoF camera vel. ${}^c\boldsymbol{\vartheta} = -\lambda \boldsymbol{J}^+ \boldsymbol{e}$

Simulations

(real experiments results are shown in Task Control section)

Camera velocities during a servo task
subject to white noise of1mm in the focal length

PBVS

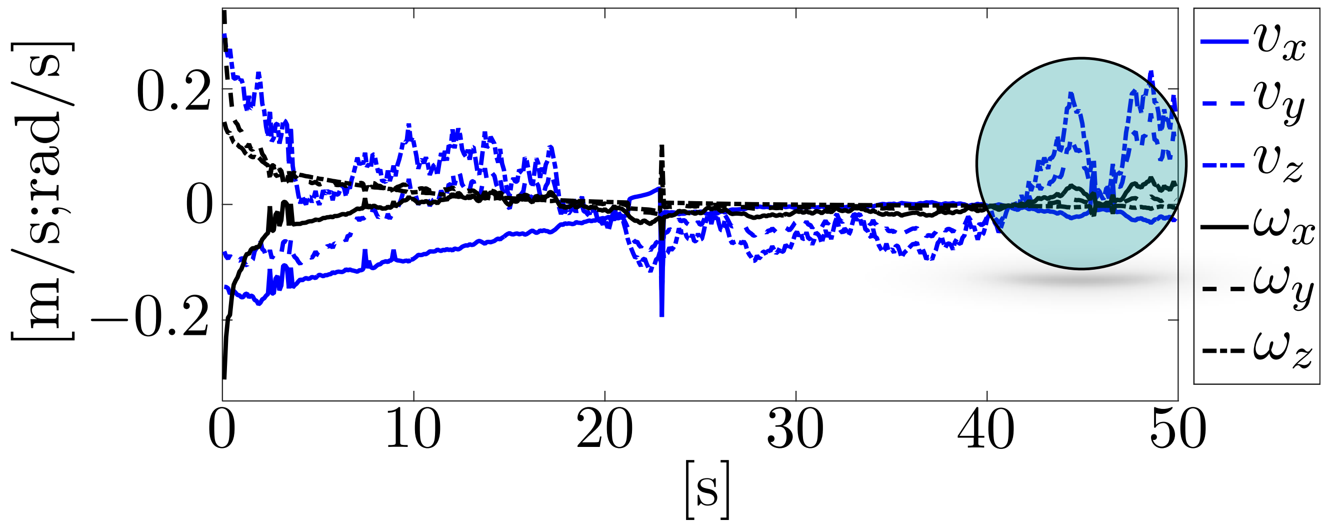

IBVS

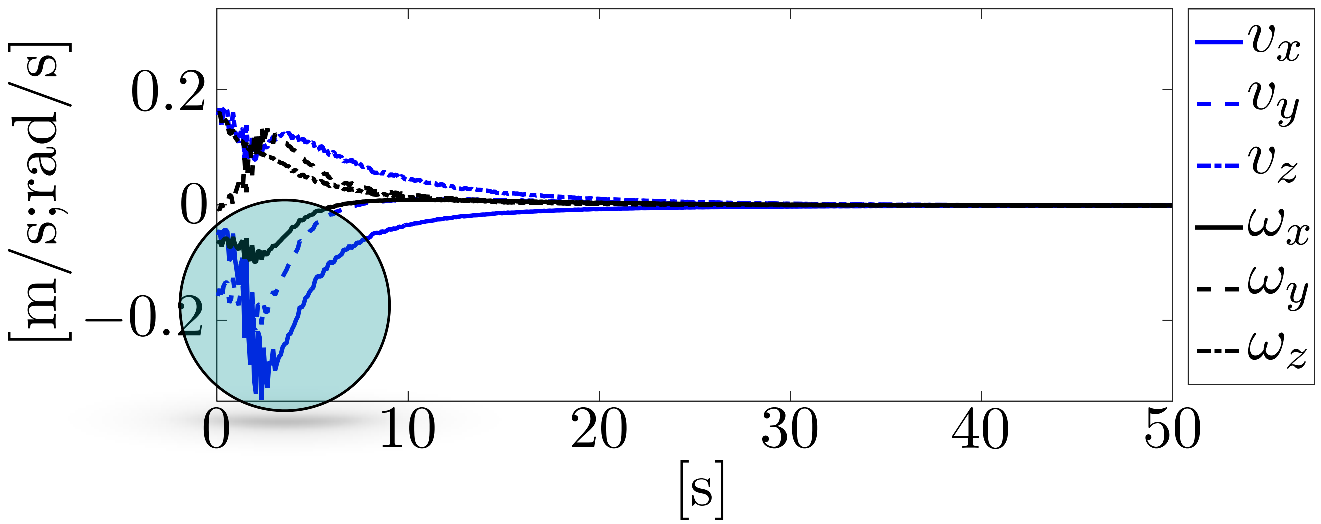

UIBVS

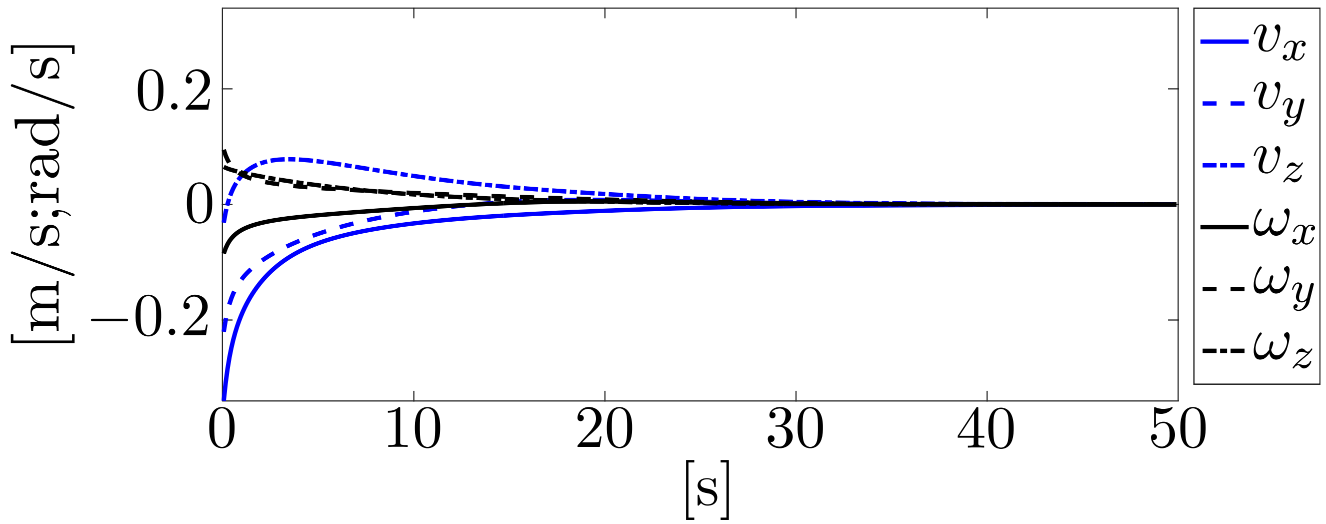

Focal length variations become undesired camera velocity references for **PBVS** and **IBVS**

Initialization error in camera focal length

Noise-free

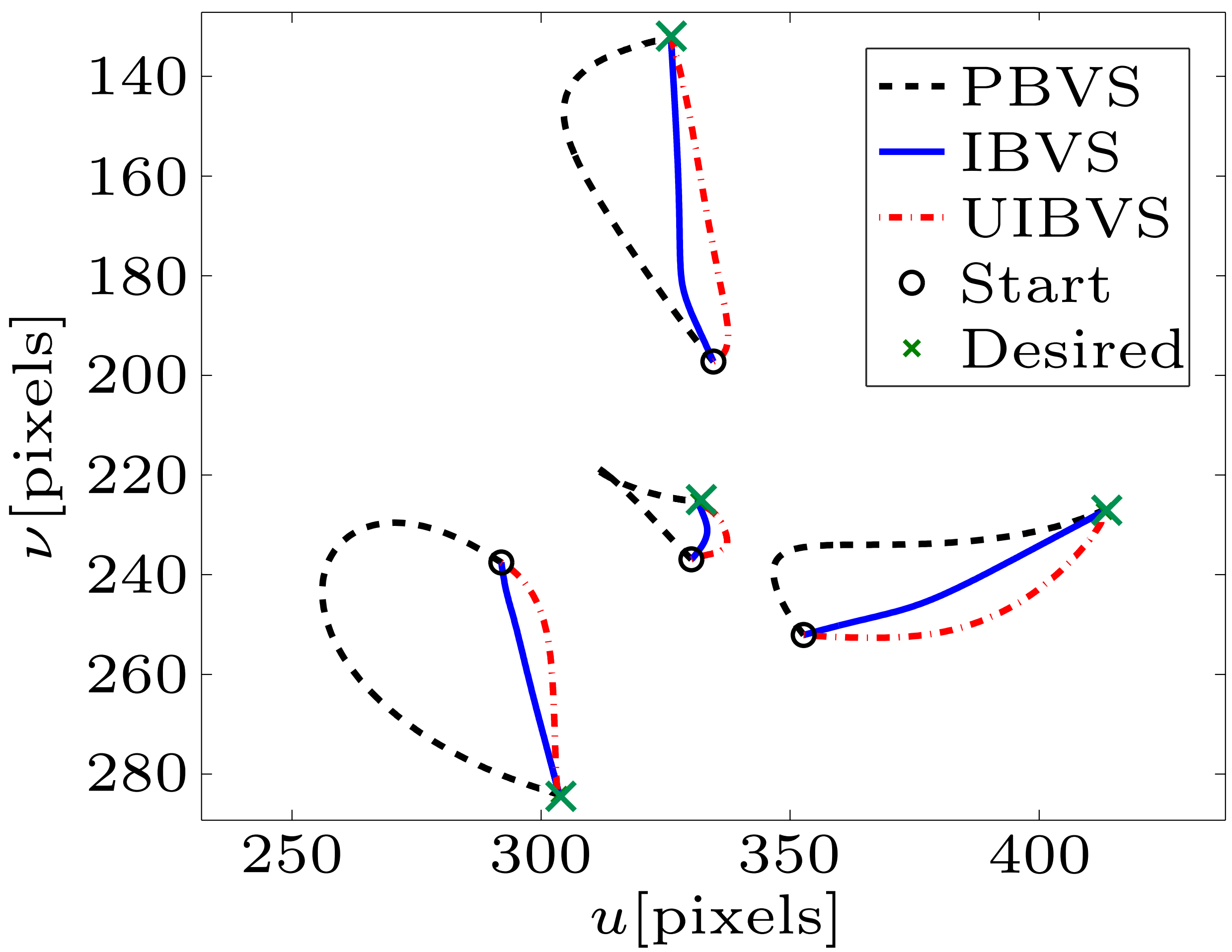

20% of error

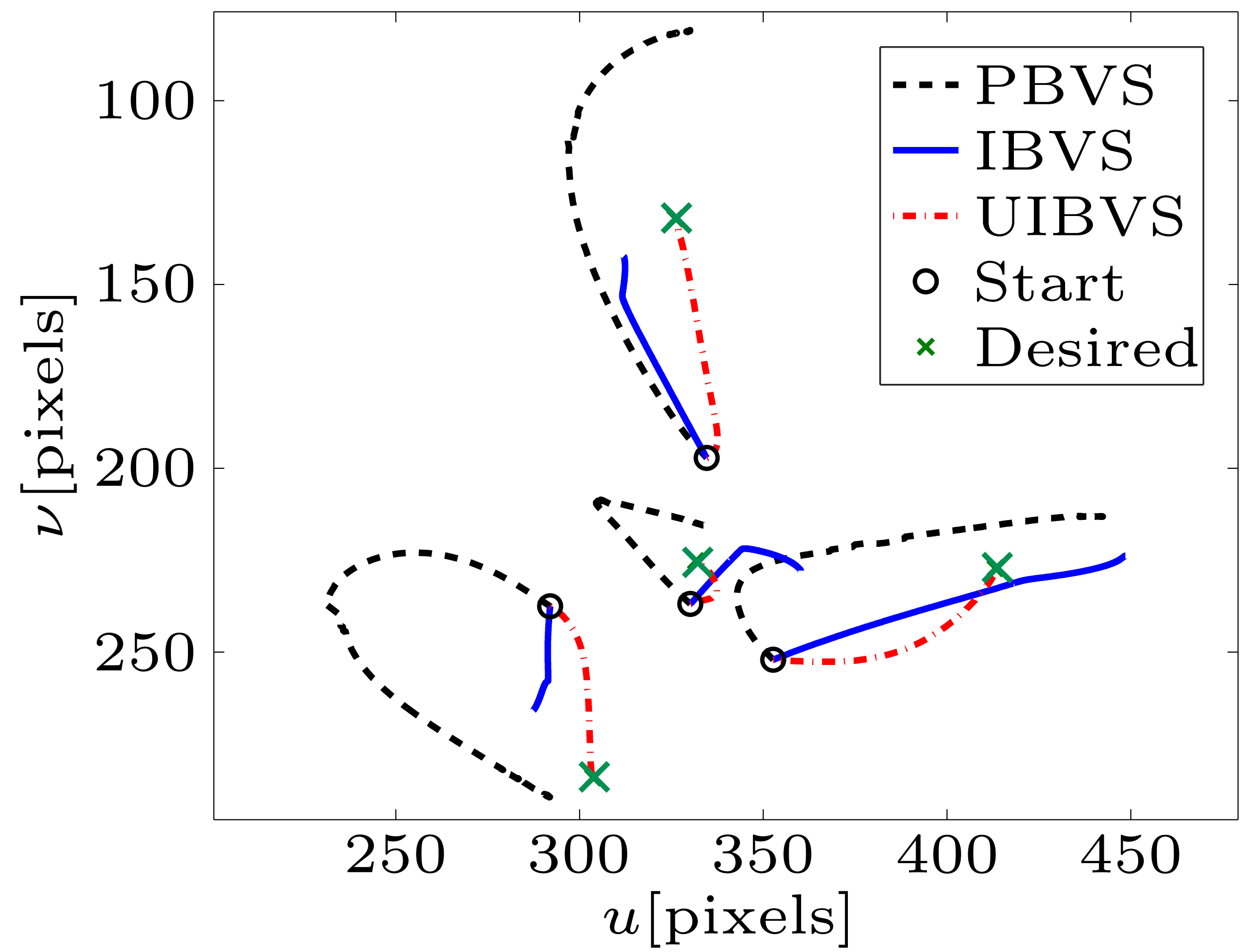

With a wrong initialization 20%
PBVS and **IBVS are unable**
to reach the desired configuration

Visual servo remarks

- New uncalibrated image-based visual servo method (UIBVS)
  - Target features parameterized with CP coordinates
  - Method to recover CP 3D coordinates and focal length
  - New calibration-free image Jacobian
  - Robustness w.r.t. focal length noise and wrong initialization

Santamaria-Navarro, A., Grosch, P., Lippiello, V., Solà, J., and Andrade-Cetto, J. Uncalibrated visual servo for unmanned aerial manipulation, 2017 IEEE/ASME Transactions on Mechatronics (T-MECH), 22(4), 1610-1621, 2017.

Santamaria-Navarro, A. and Andrade-Cetto, J. Uncalibrated image-based visual servoing, 2013 International Conference on Robotics and Automation (ICRA), pp. 5227-5232, Karlsruhe, Germany.

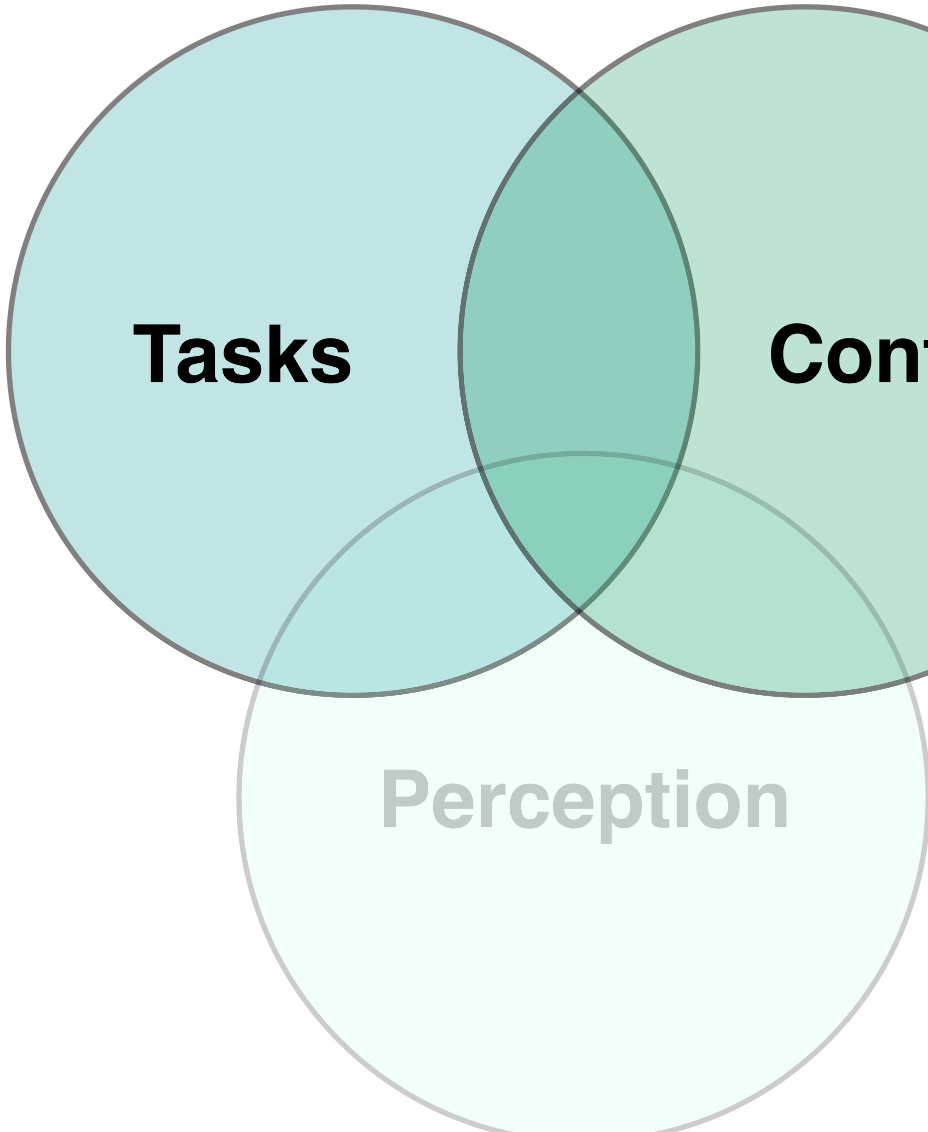

Outline

- Robot state estimation
- Visual servo control
- Task control
- Conclusions

Kinematics

$$\underbrace{{}^{c}\boldsymbol{\vartheta}}_{\text{Cam. vel.}} = \boldsymbol{J}_R \underbrace{\boldsymbol{\xi}}_{\text{Robot DoFs}} \qquad \boldsymbol{\xi} = [\overbrace{\boldsymbol{v}^\top \quad \boldsymbol{\omega}^\top}^{\text{platform}} \quad \overbrace{\dot{\boldsymbol{\gamma}}^\top}^{\text{arm}}]^\top$$

We need the robot Jacobian to map velocities from camera to joint frames

Bone breaker 1:20 (FADA-CATEC)

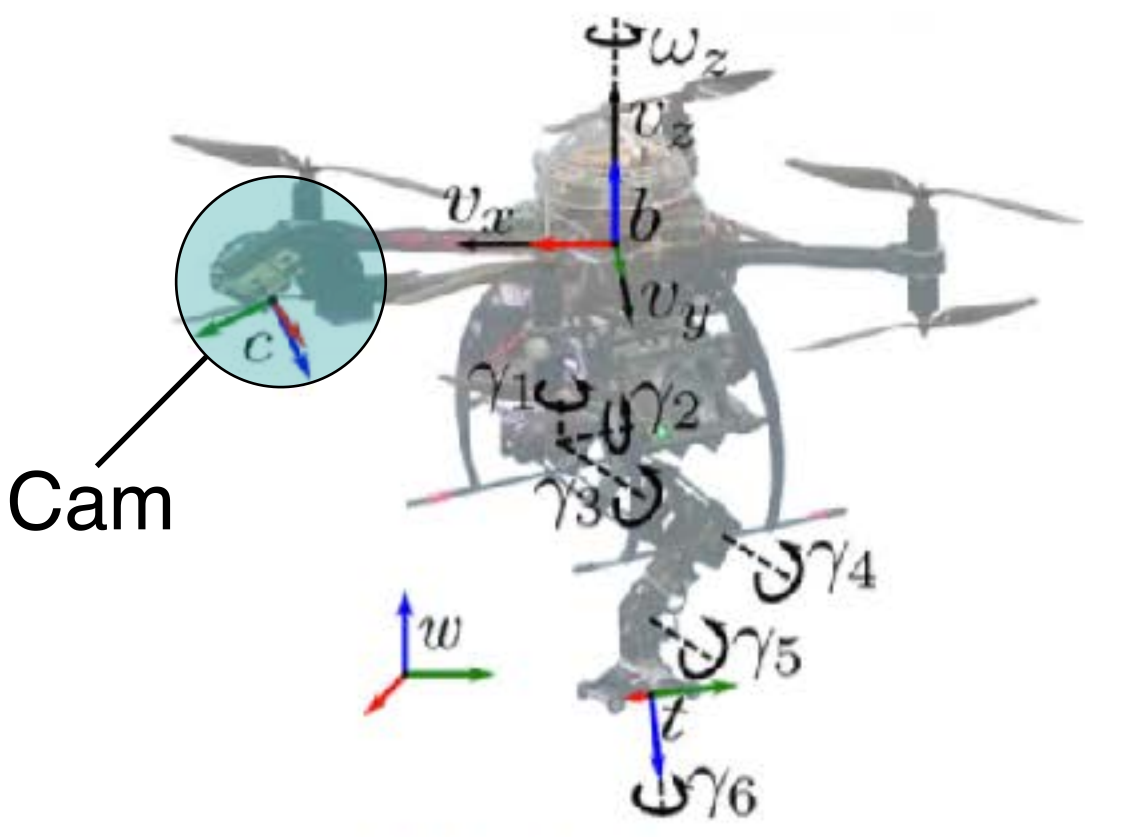

Kinton 1:10 (IRI)

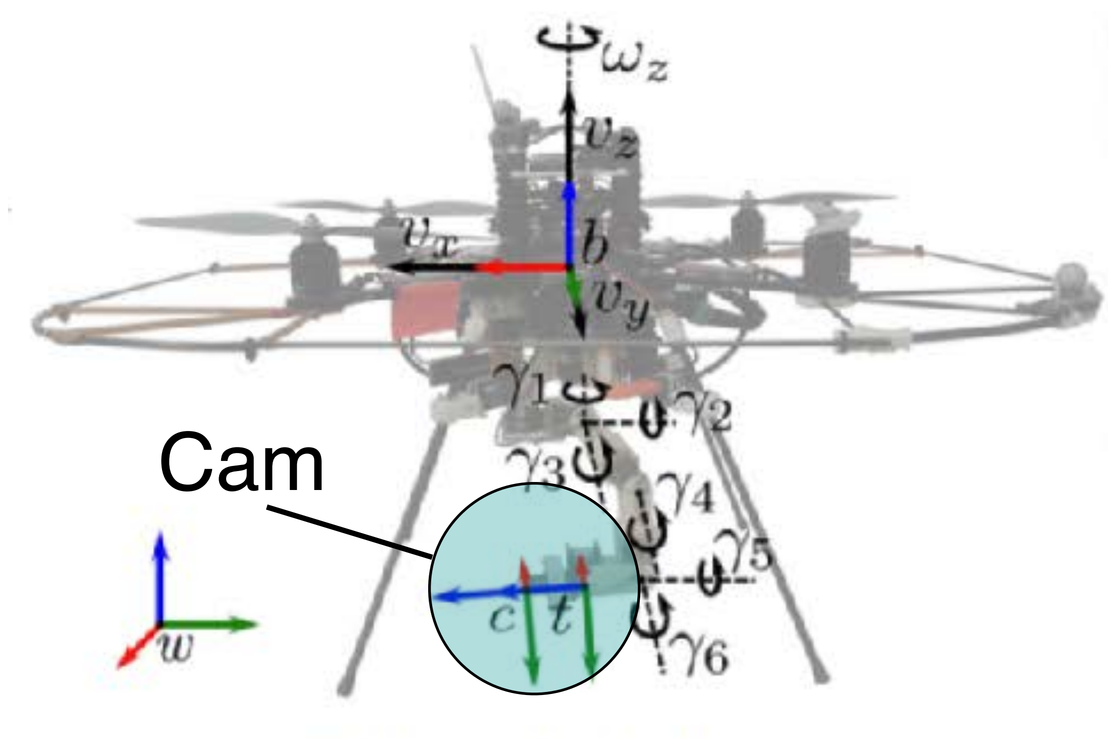

- Platform under actuation: Remove uncontrollable DoFs $\boldsymbol{\varpi}$

$$\boldsymbol{\vartheta}_C = \boldsymbol{J}_R \boldsymbol{\xi}$$

↓ split

$$\boldsymbol{\vartheta}_C = \boldsymbol{J}_R \dot{\boldsymbol{\rho}} + \overline{\boldsymbol{J}}_R \boldsymbol{\varpi} \quad \longrightarrow \quad \dot{\boldsymbol{\rho}} = \boldsymbol{J}_R^{\#} (\boldsymbol{\vartheta}_C - \overline{\boldsymbol{J}}_R \boldsymbol{\varpi})$$

Joint references ($\dot{\boldsymbol{\rho}}$)

Uncontrollable (gyros read.) ($\boldsymbol{\varpi}$)

Weighted pseudo-inverse to distribute motion ($\boldsymbol{J}_R^{\#}$)

e.g.

- Platform: large displacements
- Arm: precise movements

Task Control

Tasks

6 DoF
- Navigation
- Visual servo

→ UAMs are usually redundant (>6DoF)

We can define a set of different tasks and set priorities according to mission phases

Task combination methods
- Hierarchical control laws (x2)
- Optimization-based approach

Tasks

- Collision avoidance (obstacles or self-collisions)

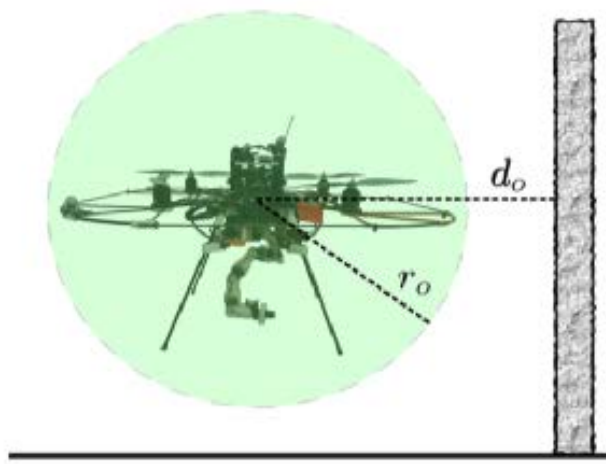

$$\sigma_0 = r_0 - ||\boldsymbol{d}_0||$$

- Visual Servo
  - Global end effector tracking: **PBVS** using global coordinates
  - Local end effector tracking: **IBVS** or **UIBVS**
  - Keeping target in camera FoV: **HVS** $\sigma_f = \boldsymbol{e}_f^\top \boldsymbol{e}_f$

- Arm CoG alignment with platform gravitational vector

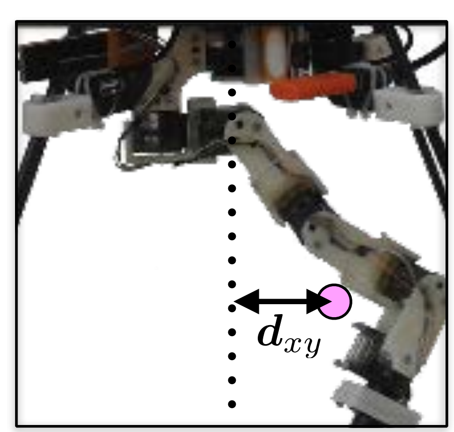

$$\sigma_g = \boldsymbol{d}_{xy}^\top \boldsymbol{d}_{xy}$$

- Reach a desired arm configuration

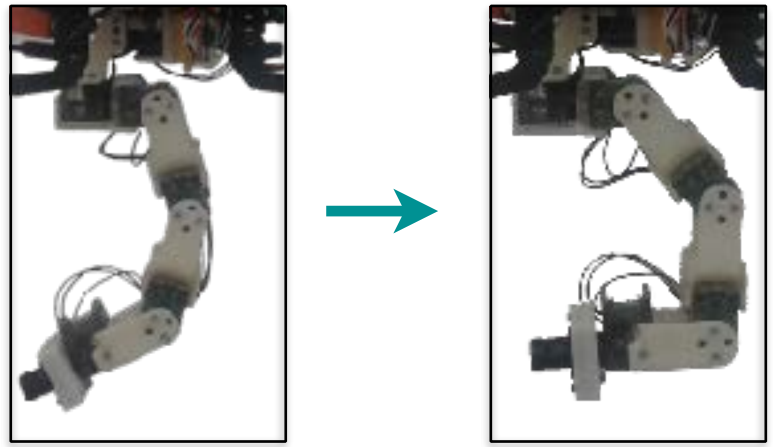

current γ desired γ^d

$$\sigma_l = (\gamma - \gamma^d)^\top \mathbf{\Lambda}_l (\gamma - \gamma^d)$$

- Maximize manipulability index

Manipulability ellipsoid

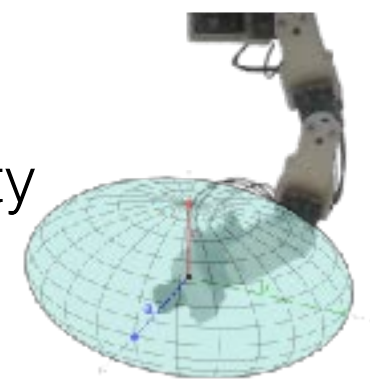

$$\sigma_m = \frac{1}{\prod_{i=1}^{r} \mu_i}$$

- Minimize velocity of specific joints
- Limit platform accelerations
- Reduce forces on platform horizontal plane

Hierarchical task control (HTPC)

- Assign priorities with the null space projection technique
- Dynamic change of task priorities

Classical HTPC

Collaboration with FADA-CATEC and UNINA

Exact tracking of the primary task while minimizing secondary task error

Null space projector

$$\dot{\boldsymbol{\rho}} = \boldsymbol{J}_0^+ \Lambda_0 \tilde{\boldsymbol{\sigma}}_0 + (\boldsymbol{J}_1 \boldsymbol{N}_0)^+ \Lambda_1 \tilde{\boldsymbol{\sigma}}_1 - \overline{\boldsymbol{J}}_{0|1} \boldsymbol{\varpi}$$

Can lose rank (algorithmic singularities) **+** Requires orthogonal or independent tasks

HTPC decoupling algorithmic singularities

Tracking of components that do not conflict with the primary task

$$\dot{\boldsymbol{\rho}} = \boldsymbol{J}_0^+ \Lambda_0 \tilde{\boldsymbol{\sigma}}_0 + \boldsymbol{N}_0 \boldsymbol{J}_1^+ \Lambda_1 \tilde{\boldsymbol{\sigma}}_1 - \overline{\boldsymbol{J}}_{0|1} \boldsymbol{\varpi}$$

Classical HTPC

Tasks

- HVS
- Arm CoG alignment
- Desired arm cfg.

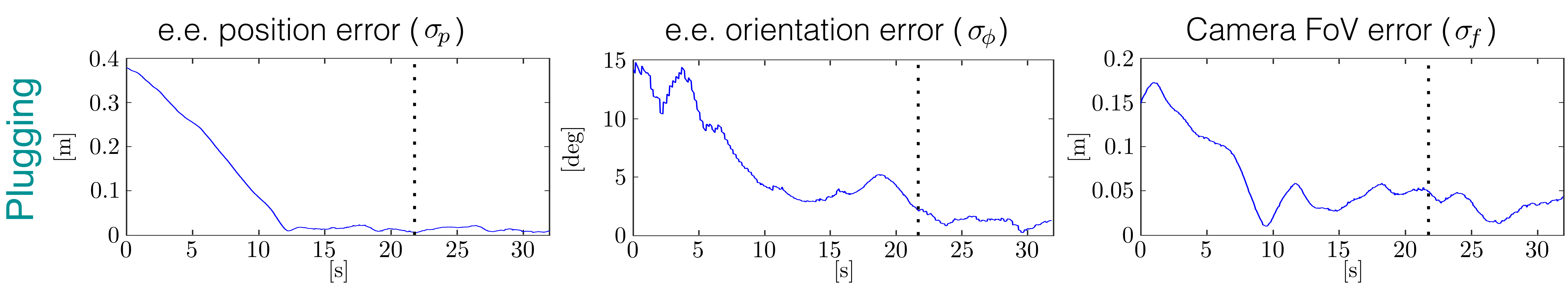

HTPC decoupling algorithmic singularities

Tasks: UIBVS + arm CoG alignment + desired arm cfg.

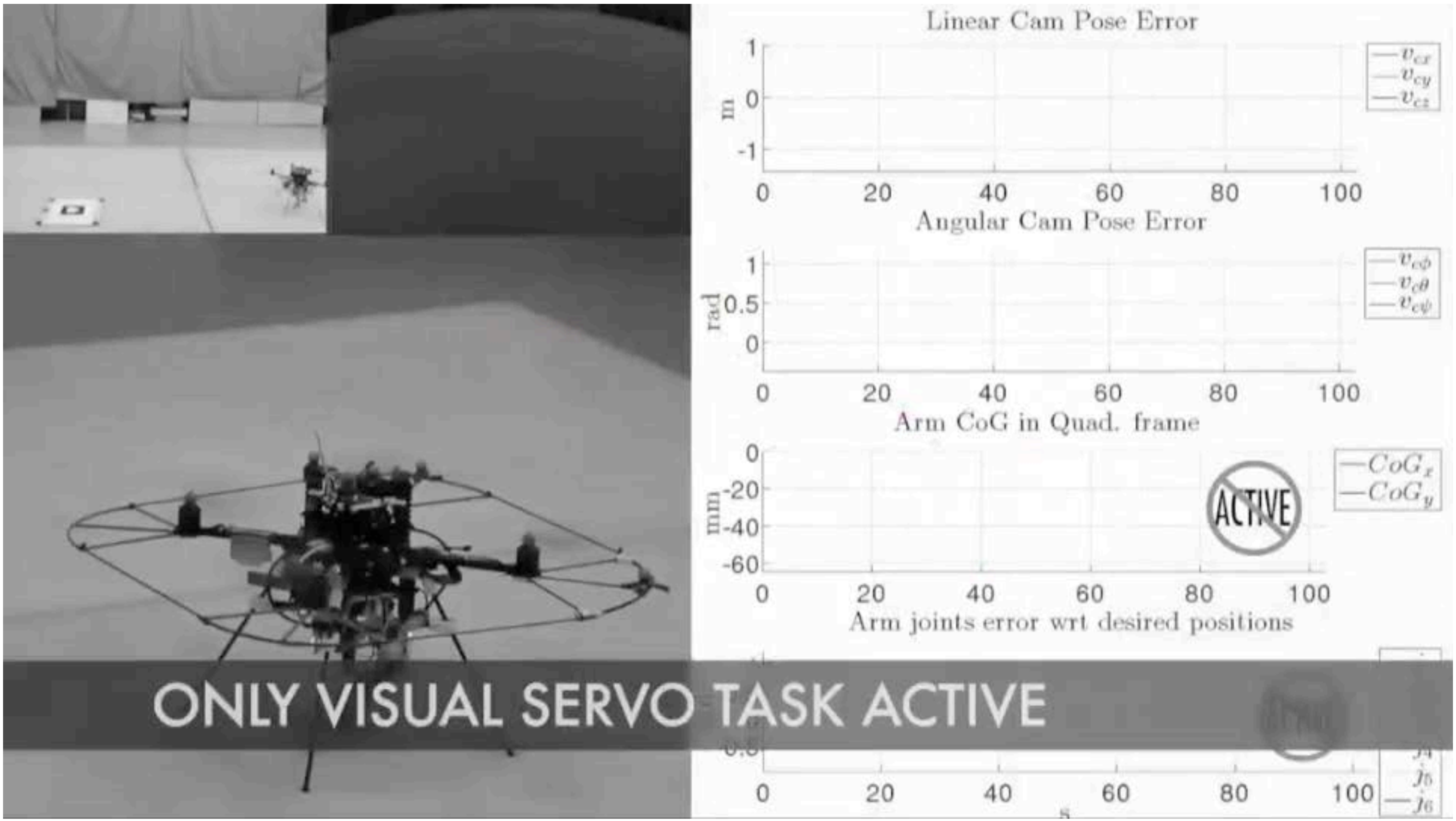

Remarks on task control

- Two configurations: onboard camera and camera at the end effector
- Task and constraints designed for UAMs
- New Task control architectures for UAMs

Santamaria-Navarro, A., Grosch, P., Lippiello, V., Solà, J., and Andrade-Cetto, J., Uncalibrated visual servo for unmanned aerial manipulation, 2017 IEEE/ASME Transactions on Mechatronics (T-MECH), vol. PP, num. 99 , pp. 1-1.

Rossi, R., Santamaria-Navarro, A., Andrade-Cetto, J., and Rocco, P., Trajectory generation for unmanned aerial manipulators through quadratic programming, 2017 IEEE Robotics and Automation Letters (RA-L + ICRA), vol. 2, num. 2., pp. 389-396.

Lippiello, V., Cacace, J., Santamaria-Navarro, A., Andrade-Cetto, J., Trujillo, M. A., Esteves, Y. R., and Viguria, A., Hybrid visual servoing with hierarchical task composition for aerial manipulation, IEEE Robotics and Automation Letters (RA-L + ICRA), vol. 1, num. 1, pp 259-266.

Santamaria-Navarro, A., Lippiello, V., and Andrade-Cetto, J., Task priority control for aerial manipulation, 2014 IEEE International Symposium on Safety, Security and Rescue Robotics (SSRR), pp. 1-6, Toyako-cho, Hokkaido, Japan.

Thank you!

Code + multimedia: http://angelsantamaria.eu

Visual Guidance of Unmanned Aerial Manipulators

Àngel Santamaria Navarro and Juan Andrade Cetto

Institut de Robòtica i Informàtica Industrial

CSIC

UPC

ARCAS

AEROARMS